Open access • Journal Article • DOI:10.1109/CEEJ.1979.6593929

Digital baseband processing of a Mills' cross array antenna

Simon Haykin, H. Rahman

Institutions: McMaster University

Published on: 01 Oct 1979 - Canadian Electrical Engineering Journal (IEEE)

Topics: Baseband processor, Baseband, Line code, Modulation and Digital signal processor

DIGITAL BASEBAND PROCESSING OF A MILLS' CROSS ARRAY ANTENNA

by

(C) MD. HABIBUR RAHMAN, B.Sc.Eng., M.Sc.Eng.

A Thesis

Submitted to the School of Graduate Studies

in Partial Fulfilment of the Requirements

for the Degree

Master of Engineering

McMaster University

September, 1979

DIGITAL BASEBAND PROCESSING OF A MILLS' CROSS ARRAY ANTENNA

MASTER OF ENGINEERING (1979)
(Electrical Engineering)

McMASTER UNIVERSITY
Hamilton, Ontario

TITLE: Digital Baseband Processing of a Mills' Cross Array Antenna

AUTHOR: Md. Habibur Rahman,

B.Sc.Eng. (Bangladesh University of Eng. & Tech., Dacca)

M.Sc.Eng. (Bangladesh University of Eng. & Tech., Dacca)

SUPERVISOR: Dr. Simon Haykin

NUMBER OF PAGES: x, 101

ABSTRACT

A digital signal processor, operating at baseband, is described for the scanning of a Mills' cross array antenna. The processor uses time modulation to scan the pencil beam produced by the array in a raster-like fashion over the prescribed sector. The scheme uses within-pulse scanning in order to avoid the loss of power in the fan beams outside the area covered by the pencil beam. This processor provides flexibility in applying different types of aperture distribution to modify the side-lobe structure of the antenna pattern. It provides a simple means for changing the scanning rate of the array.

The different types of scanning technique are reviewed briefly. A detailed mathematical analysis of time modulation scanning technique is presented. Experimental results are included to demonstrate the practical feasibility of the digital baseband processor for scanning the Mills' cross array antenna along prescribed look directions inside the visible region of interest.

ACKNOWLEDGEMENTS

The author gratefully acknowledges the help and guidance given to him by his supervisor, Dr. Simon Haykin throughout the preparation of this work. He wishes to thank Dr. C.R. Carter, as well as the research personnel of the Communications Research Laboratory at McMaster, for their co-operation.

Financial support of the work by the Department of Electrical Engineering at McMaster University is gratefully acknowledged. The author wishes to thank Miss P. Dillon of the Word Processing Centre for her assistance in the typing.

Finally, the author wishes to thank his wife, Paulin, for her encouragement, constant understanding and support throughout the whole period of this work.

TABLE OF CONTENTS

TABLE OF CONTENTS (continued)

LIST OF FIGURES

LIST OF FIGURES (continued)

LIST OF FIGURES (continued)

LIST OF TABLES

CHAPTER 1

INTRODUCTION

1.1 Historical Review

The use of a phased-array antenna in radar offers the unique feature of being able to achieve, in a single radar system, the operations of search, track, and discrimination of many high-velocity targets simultaneously. In those radar applications which require the use of a pencil beam to provide information in both azimuth and elevation, the most versatile solution is to use a planar array. However, owing to the large number of radiating elements which a practical planar phased-array antenna would require and the duplication of equipment in each channel for processing the received signal, the total cost of implementing such a system can be quite expensive. A substantial reduction in cost can be achieved, whilst retaining the high resolution capability of a conventional planar array, by using the Mills' cross array [1]. In this structure, all but two linear arrays of elements (arranged to be at right angles to each other) are eliminated from a planar phased-array antenna.

A Mills' cross-array involves the use of multipli-

cative signal processing in order to achieve the desired high resolution. Specifically, the elemental outputs of the 2 arms of the array are weighted appropriately and then added, and the resulting output signals from the 2 arms are applied to a cross-correlator. The output of this correlator has the equivalent effect of a two-dimensional pencil beam at the intersection point of the two fan beams produced by the 2 perpendicular arms of the array. The array may consist of dipoles, in which case the pattern produced by each arm of the array would be directive in the plane containing the axis of the arm and broad in the plane at right angles to it. Alternatively, the elements may consist of parabolic dishes or any other convenient radiating elements. The Mills' cross array is most appropriate for use in those applications in which the sources (or targets) of interest are uncorrelated, as is the case in radio astronomy or a radar system that does not suffer from multipath. The reason for this is that if correlated signals (originating from different directions) are received simultaneously by both arms of the array, the system will recognize them as a signal originating from the central main beam of the array.

The principle of antenna pattern multiplication to achieve a pencil beam was first demonstrated in 1953 by Mills and Little [1]. In this structure, the arms of the

cross are 120 ft. in length and consist of a line of folded dipoles which are fed from a twin wire transmission line. It operates at a frequency of 97 MHz resulting in a beam-width of 8°. The Mills cross at Fleurs near Sydney, Australia has been successfully put into operation. Each arm of the cross consists of 500 half-wave dipoles extending over 1,500 feet. The resolution is 49 min. of arc at 85 MHz and the beam can be tilted about 45° on either side of zenith by adjusting the relative phases of the dipoles. In the meantime, a number of giant radio telescope, based on this principle, have been constructed in different parts of the world. The Australian cross [2] consists of two parabolic cylinders with line feeds arranged as a cross. Each arm of the cross is 1600 x 13 meters. It operates at 408 MHz and 111.5 MHz. The Russian Mills Cross [3] has a similar mechanical design. Each cylinder is 1000 x 40 meters with focal distance 14.5 meters. The cross is designed for operation at meter wavelengths (50 - 200 MHz). The Italian Mills' Cross [4] is of a similar design except for the north-south arm. It operates at a frequency of 408 MHz. The east-west arm is 1190 x 30 meters while the north-south arm consists of 96 parabolic cylinder reflectors, each having 42 x 8 meters and spaced 11.5 meters apart. In all these cross-type antennas, the elements of the crosses are made of sections of parabolic cylinders. The use of

identical sections greatly reduces the cost for construction. Wislez and Gonze [5] have indicated the application of the Mills' cross to both solar mapping and radio source localization. The use of a Mills' cross array for radar applications has also been described by Slattery [6] and Davies [7].

1.2 Digital Baseband Processor

In this thesis, we describe the digital implementation of a baseband processor used in conjunction with a Mills' cross array antenna system for radar application. The scanning of the pencil beam, produced by the Mills' cross, in a prescribed sector is achieved by sweeping the individual fan beams generated by the two arms of the cross at different speeds. One approach to forming the fan beam and steering it at a desirable speed would be to multiplex the element signals into a single channel by using a technique known as element signal multiplexing. Examples of this technique are frequency modulation scanning [8] and time modulation scanning [9]. In this thesis, we will focus attention on the use of the time modulation scanning as it is rather well-suited for practical implementation using digital hardware.

The purpose of the digital processor is two fold: (1) to perform the cross-correlation required for

construction of the pencil beam and (2) to provide a continuous scanning capability of the pencil beam in a prescribed sector by using time modulation [9]. The scheme uses within-pulse scanning in order to avoid loss of power in the fan beams outside the area covered by the pencil beam. Within-pulse scanning is essentially a sampling technique, whereby all targets (i.e. the whole scanning sector) are scanned once per transmission pulse length. Thus, targets at all ranges are sampled during one repetition period.

The processor offers the following advantages:

(1) It eliminates the need for phase shifters which can be expensive.

(2) It provides flexibility in applying different types of aperture illumination to modify the sidelobe structure of the antenna pattern.

(3) It provides a simple means for changing the scanning rate of the array.

(4) It uses digital hardware for the processing of base-band signals consisting of in-phase and quadrature components.

1.3 Organization of the Thesis

Before going into the details of the proposed digital baseband processor, it is instructive to present a brief

review of different beam forming and steering techniques. Chapter 2 reviews the beam forming and steering techniques available in literatures and then gives a detailed mathematical analysis of time modulation scanning technique. In Chapter 3 we describe in detail the experimental system. In Chapter 4, we present some experimental results obtained with an 8 x 8 Mills' cross phased-array antenna and compare them with theory. Finally, in Chapter 5, we present conclusions of the thesis.

CHAPTER 2

SCANNING TECHNIQUES

2.1 Introduction

Mechanically scanned antennas were employed almost exclusively in the radar systems of World War II and are still being used in the majority of operational radar systems today. However, new requirements for radar systems (such as rigidity and shock resistance of the antenna structure, volumetric rapid scanning of large antennas, and avoidance of any mechanical motion in the radar system) have led to a renewed interest in electronically scanned antennas in which the antenna stays fixed in space and the radar beam is moved by introducing proper linear progressive phase shifts along the length of the antenna. Such an antenna is called a "phased array". A phased array is so called because a number of antennas are interconnected to radiate or receive coherently, and, by controlling the relative phase of the signals between antenna elements, a beam can be formed and steered over a large sector. Phased arrays can provide scanning patterns and scanning rates which are impossible to attain with mechanically positioned directional arrays. There are a number of ways in which the

progressive phase shifts along the length of array can be varied in accordance with the beam desired.

This chapter presents a brief review of the different scanning techniques of phased arrays, and then gives a detailed mathematical analysis of the time modulation scanning on which we will concentrate in this thesis.

2.2 Phase Scanning

The relative phases between the radiating elements in the array antenna determine the position of the main beam which points in a direction that is normal to the phase front. If the phases are fixed, the antenna radiation pattern is also fixed. Scanning of the beam formed by an array can be accomplished by mechanically moving the entire array-antenna structure. However, in a phased array, the beam can be steered by individual control of the phase of excitation of each radiating element. This is indicated in Fig. 2.1. Specifically, the pattern of the phased-array antenna may be steered to an angle θ by applying linearly progressive phase increments from element to element, so that the phase between adjacent elements differs by $x = (2\pi/\lambda)\, d \sin\theta$ where, d is the interelement spacing, θ is the angle with normal to the antenna structure and λ is the operating wavelength. The phase shifters are employed in order to obtain the incremental phase shift x. Phased-array

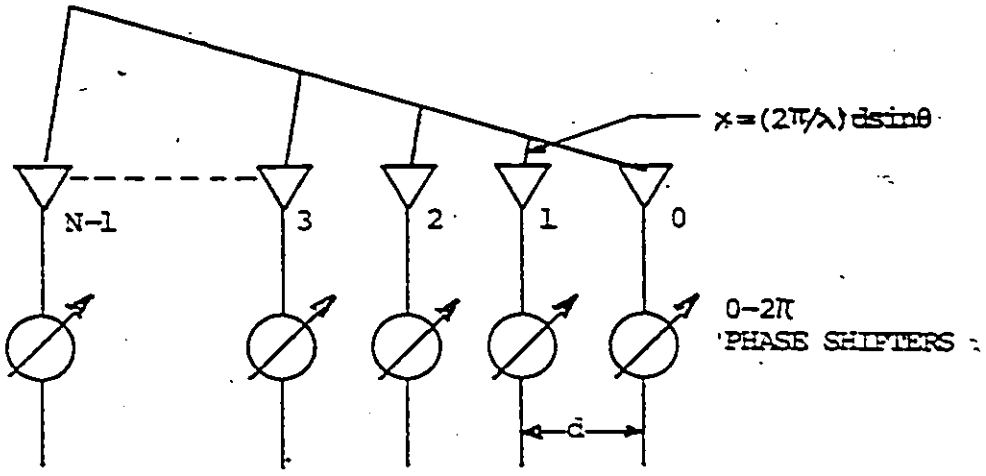

Fig. 2.1 Phase scanning array.

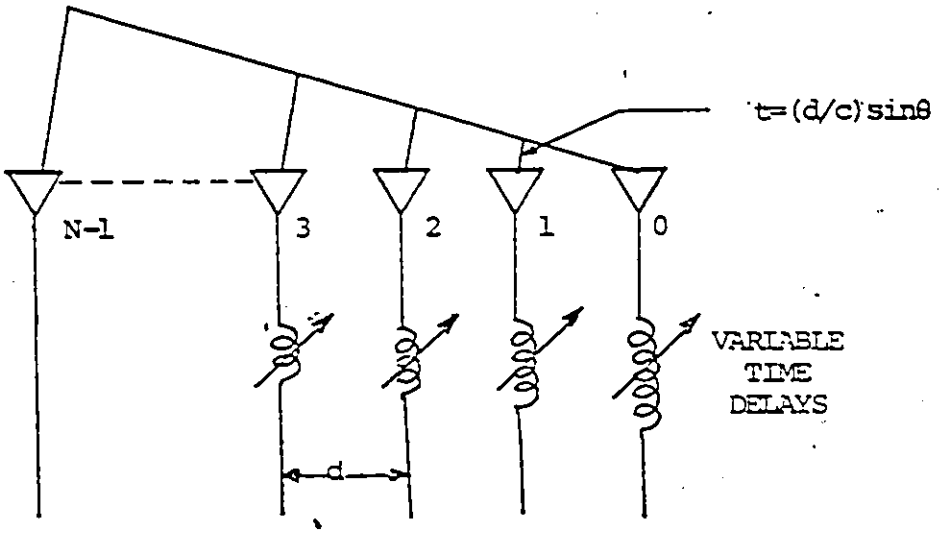

Fig. 2.2 Time-delay scanning array.

antenna can have large number of elements, with a phase shifter for each element; therefore, performance and cost of the array antenna are strongly affected by the performance and cost of the phase shifters. The phase shifters [10] are electronically actuated to permit rapid scanning and are adjusted in phase to a value between 0 and 2π. From the expression of the incremental phase shift $x = (2\pi/\lambda)\, d \sin\theta$, it is obvious that if the phase x is constant with frequency, the scan angle θ is frequency-dependent such that $(\sin\theta)/\lambda$ is constant. Thus the phase scanning is seen to be dependent on the operating frequency.

2.3 Time-delay Scanning

The problem of dependence of the phase scanning on frequency is overcome by using delay lines [11] instead of phase shifters as indicated in Fig. 2.2. This provides an incremental delay from element to element of $t = (d/c) \sin\theta$, where c is the velocity of propagation. Phasing circuits capable of providing true time-delays are required for this purpose. These circuits are normally operated at relatively low power levels and consist of a number of transmission line lengths that can be switched into or out of the paths to the array elements. The line lengths may be made in binary increments. The combination of circuit elements for producing a step in time delay is called a time-delay bit.

Thus the individual time-delay circuits are normally too complex to be introduced in each radiating element. A reasonable compromize in case of a large phased array may be reached by adding one time-delay network to a group of elements that have phase shifters.

2.4 Frequency Scanning

The design of radar systems using frequency scanning antennas began in the early 1950's when microwave power generation progressed to the point where high power sources capable of variable frequency output were developed. A simple and effective method of changing the radiated beam direction is to change the operating frequency in an antenna feed system composed of frequency sensitive phase shifters. A phase shifter in this category is simply a length of transmission line chosen to meet the design requirements. A frequency-scanned antenna [12] may be represented by the series-fed array shown in Fig. 2.3 with fixed length of transmission line connecting the elements. The total phase through a fixed length ℓ of transmission line is $(2\pi f\ell/c)$ and thus a function of frequency f. The lines connecting adjacent elements of the series-fed frequency-scanned array of equal length are chosen so that the phase at each element is the same when operating at the center frequency f_o. When the frequency is exactly f_o, the beam points in the

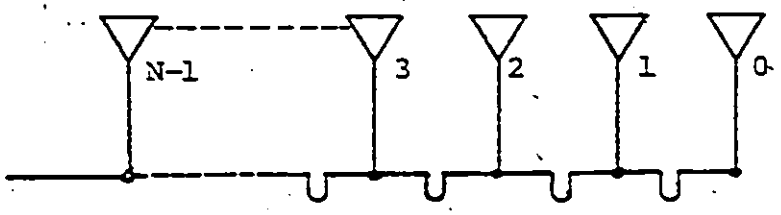

Fig. 2.3 Frequency scanning array .

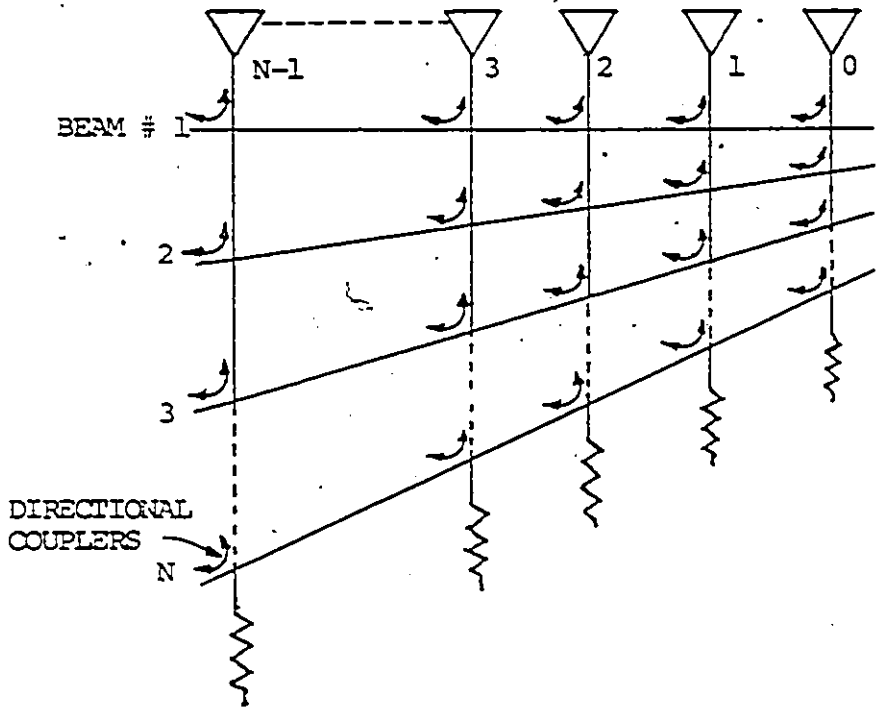

Fig. 2.4 Blass-type scanning array .

direction normal to the array plane. As the frequency is increased above f_o, the phase through each length of transmission line increases and the beam rotates to one side. At a frequency below f_o, the beam moves in the opposite direction. The implementation of a frequency-scanned array radar is relatively straight forward in principle.

The principle has been applied to develop many different forms of antenna scanning. For example, a fan beam results if a line source of this type illuminates a horn aperature. If the line source illuminates a parabolic cylinder, on the other hand, a one-dimensional scanning pencil beam is produced. Volumetric coverage may be achieved in the latter case by a combination of frequency scanning and mechanical rotation of the antenna in the orthogonal plane.

2.5 Multiple Beam Forming and Switching

Multiple beam forming systems consist of networks that generate or, more usually, receive simultaneous beams from an aperture, with each beam having the gain and beam-width of the whole antenna. One or more beams are selected by switches. On receiving, the total number of beams that may be processed simultaneously is limited primarily by the number of elements that may be made available. A typical

multiple beam forming of this type developed by Blass [13] is shown in Fig. 2.4 in which each intersection of lines represents a directional coupler. The phase shift of each length of line is represented by the physical line length. The beams produced are stationary in space and overlap at about 4 dB points. Another beam forming network, described by Butler [14],[15] contains hybrid couplers and fixed phase-shifters. This is indicated in Fig. 2.5 in which an 8-element array forms eight orthogonal beams lying to the right and left of broadside direction. The terminals have been labelled to identify the pertinent beams. The required microwave network has 2N ports and is matched at all ports. The N outputs on one side of the network that are excited by any of the N inputs on the other side possess a progressive phase characteristic that is a function of the input. The basic building block in the microwave network for multiple beam generation is the hybrid junction which can provide two overlapping beams from a two-element array. There are various configurations which provide hybrid operation.

A single hybrid junction supplies rudimentary multiple-beam operation from a two-element array. The significance of the element, however, lies in its use as a building block for arrays with more elements and beams. Figure 2.5 indicates the feed system for eight elements and the pattern for extending the number to any power of two is

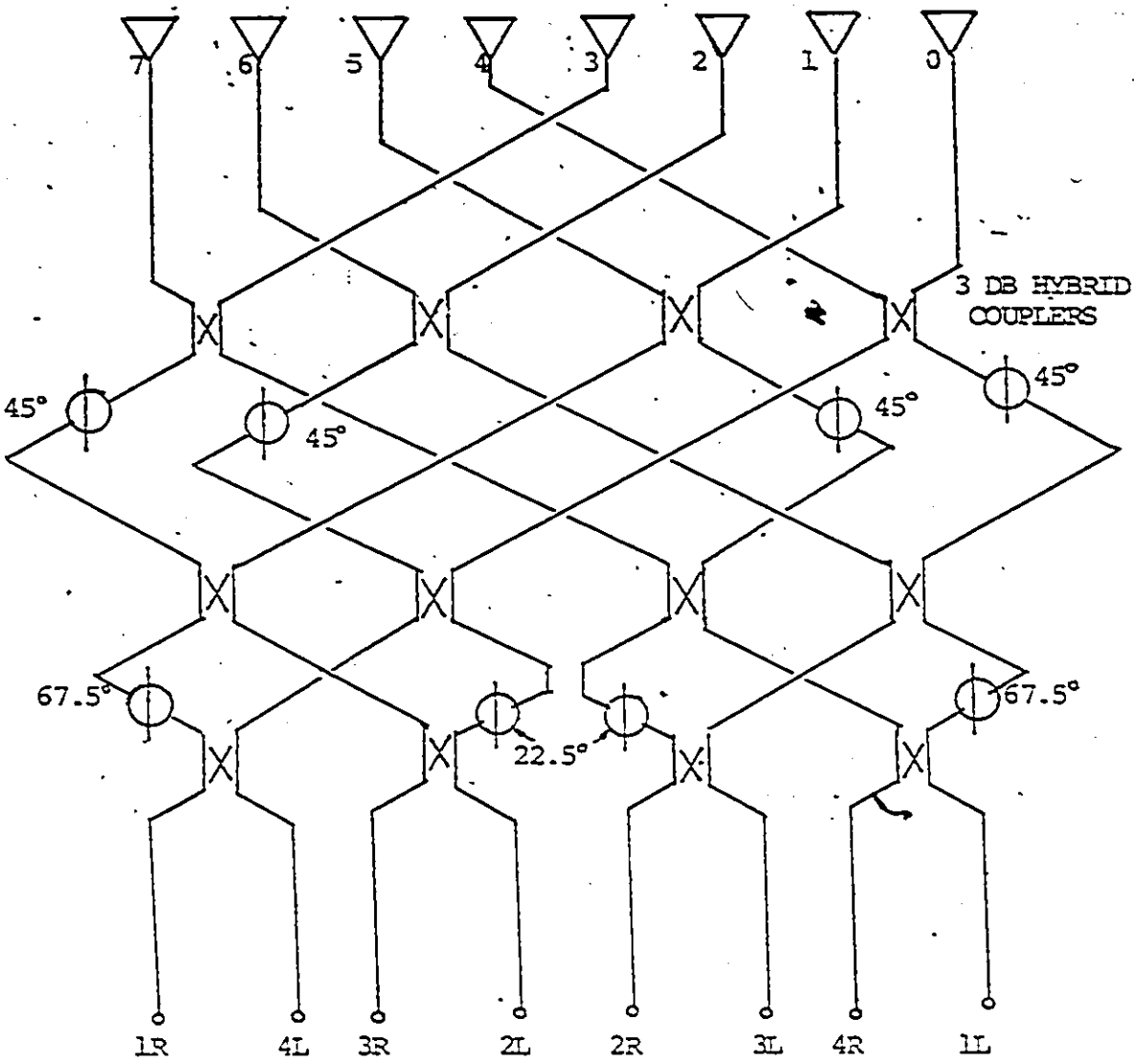

Fig. 2.5 Butler-matrix network for 8-elements array.

rather obvious. The critical aspects of the arrangements are the interconnections among the hybrids and to the elements and the added phase-shifts. All transmission lines in a given cross-section are assumed equal in length except for the phase shifters.

The principal limitation on the use of hybrids is the restriction of the number of elements to powers of two. The alternative to this difficulty is to find more building blocks. An additional limitation on the use of small building blocks is the great number that are required to feed large arrays.

2.6 Modulation Scanning

In a phased array radar system, the classical methods of beamforming and beamsteering use either elemental control elements i.e. controllable phase shifters or time delay elements or element interconnection matrices which produce a number of simultaneous beam outputs. When, however, it is required to scan the beam of the array in the receiver part of system continuously and rapidly, we may use a class of beam forming and steering technique known as modulation scanning technique which includes frequency modulation scanning [8] and time modulation scanning [8],[9] as special cases. Figure 2.6 shows the block diagram of an array signal processing receiver using modulation scanning. In

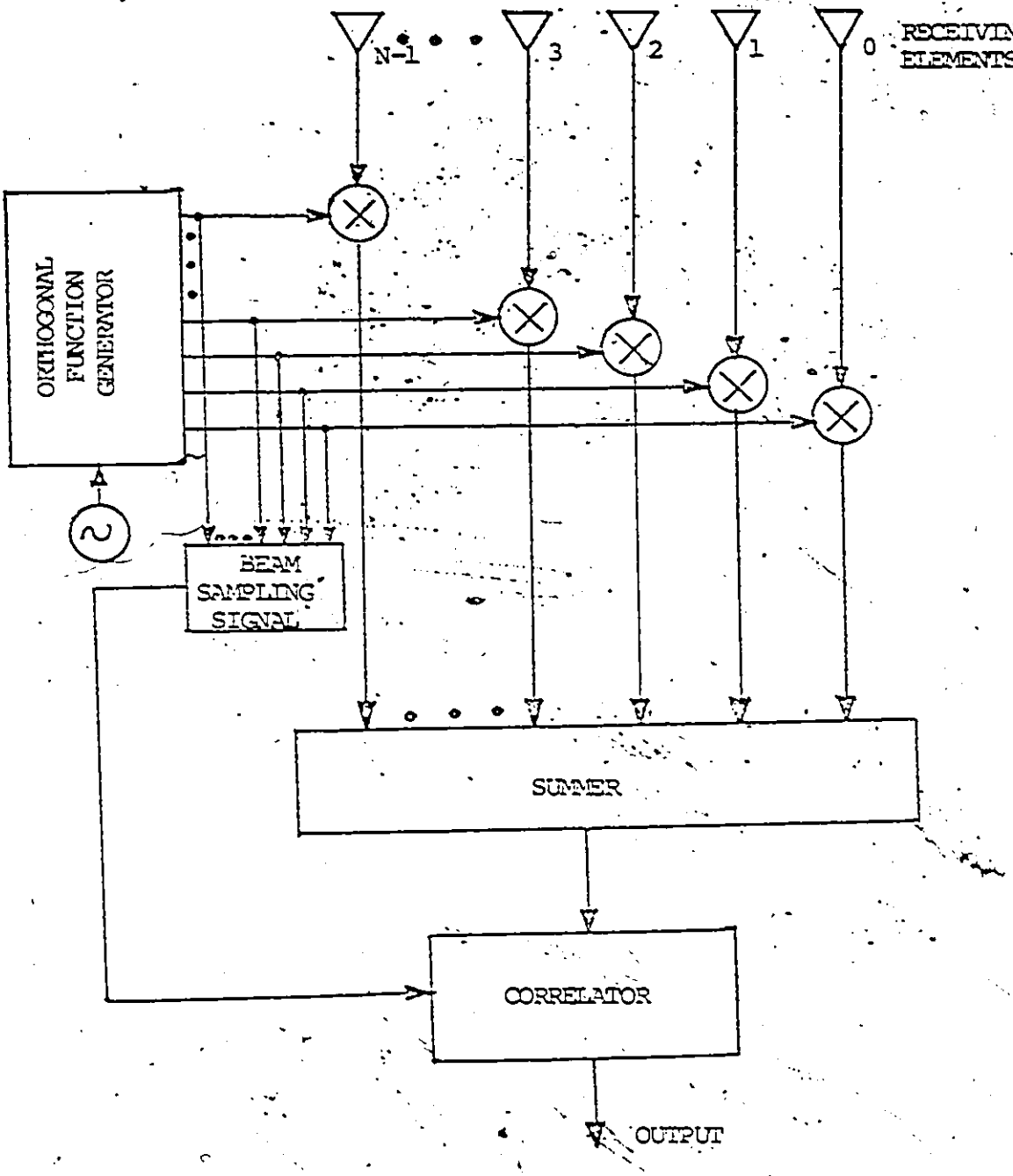

Fig. 2.6 General schematic diagram of modulation scanning array.

such a system, the received signal for each element of the array is multiplied by a corresponding component selected from a set of orthogonal functions. The choice of a particular set of orthogonal functions determines the type of scanning modulation used. The contributions thus obtained from various radiating elements of the array antenna are combined in a multiplexer to produce a main beam that scans continuously with time at a rate determined by the basic period of the set of orthogonal functions. Finally, the multiplexed signal is cross-correlated with a beam sampling signal to steer the beam to a desired direction as specified by the beam sampling signal.

In a frequency modulation scanned system, the received element siganls of the array antenna are frequency multiplexed by means of a set of scanning local oscillator signals which are spaced by a fixed frequency interval equal to the reciprocal of the pulse duration of the transmitted radar signal, thereby producing a time-multiplexed beam signal. On the other hand, in a time modulation scanned system, the received element signals of the array antenna are multiplexed in time so as to produce a frequency multiplexed beam signal. In effect, the frequency modulation and time modulation scanning techniques are the dual of each other. In this thesis, we will concentrate on the time modulation scanning as it forms the basis of the

digital baseband processor for scanning the array.

2.7 Mathematical Analysis of Time Modulation Scanning

The aperture illumination of an array antenna affects the spatial distribution of the radiated or received energy. In the time-modulation method of scanning an array, developed by Shanks [8], the aperture illumination is modulated in a periodic manner by multiplexing the received element signals of the array so as to produce a frequency-multiplexed beam signal. Specifically, each element of a linear array consisting of N elements is progressively switched on for a time T/N and then switched off for the remainder of the period, where T is the period of the periodic aperture illumination. The procedure is illustrated in Fig. 2.7 for the case of N = 8. In the implementation described by Shanks RF switches were used, whereas in the processor described in this thesis the switching operations are performed at baseband using digital hardware.

The block diagram of an array signal-processing receiver employing time modulation scanning is shown in Fig. 2.8. The band-pass signal, centered at the transmitted radio frequency, which is received by each element of the array antenna is first of all converted into its equivalent baseband (low-pass) form [16]. This is achieved by applying

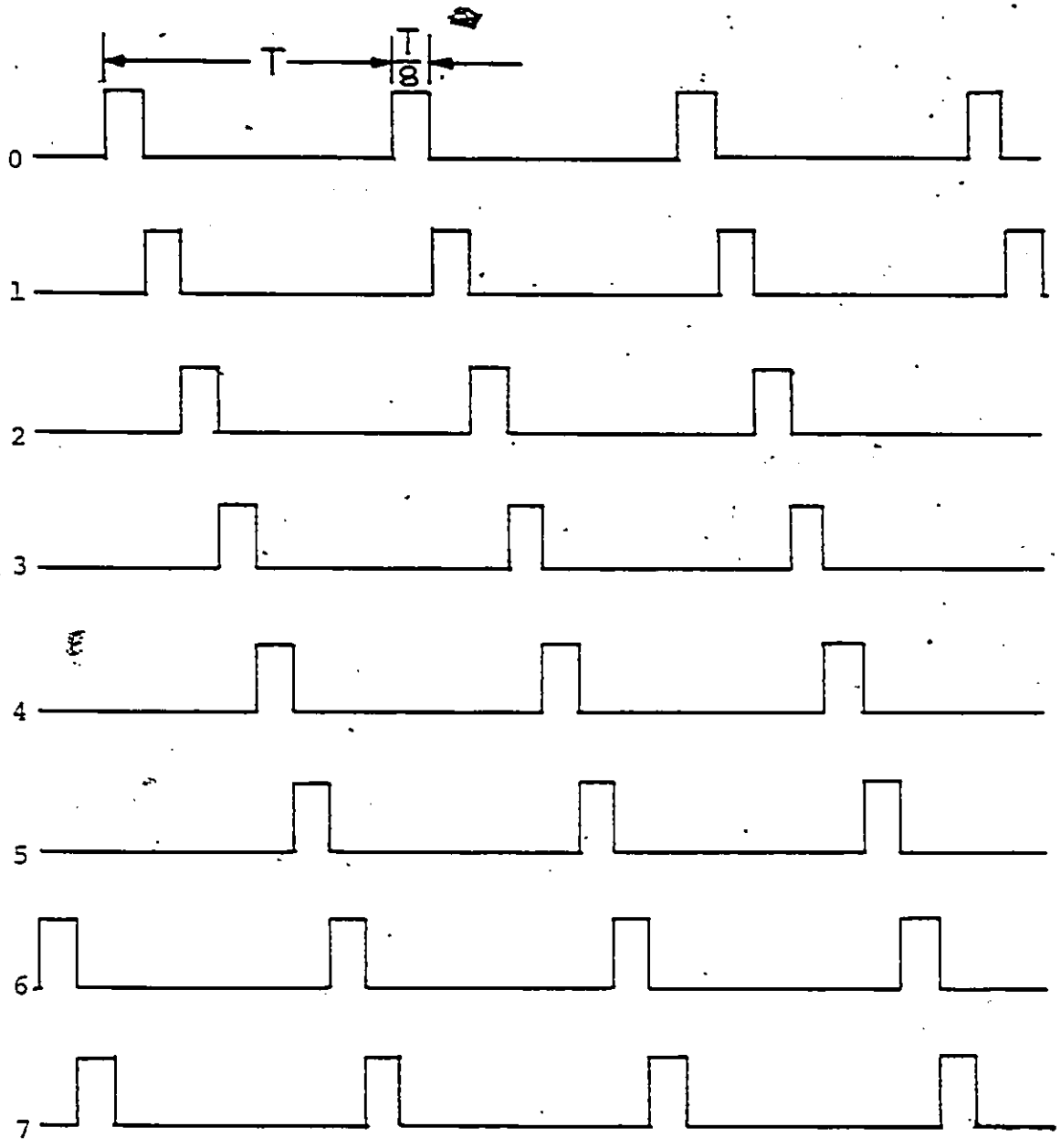

Fig. 2.7 Time-multiplexed signals

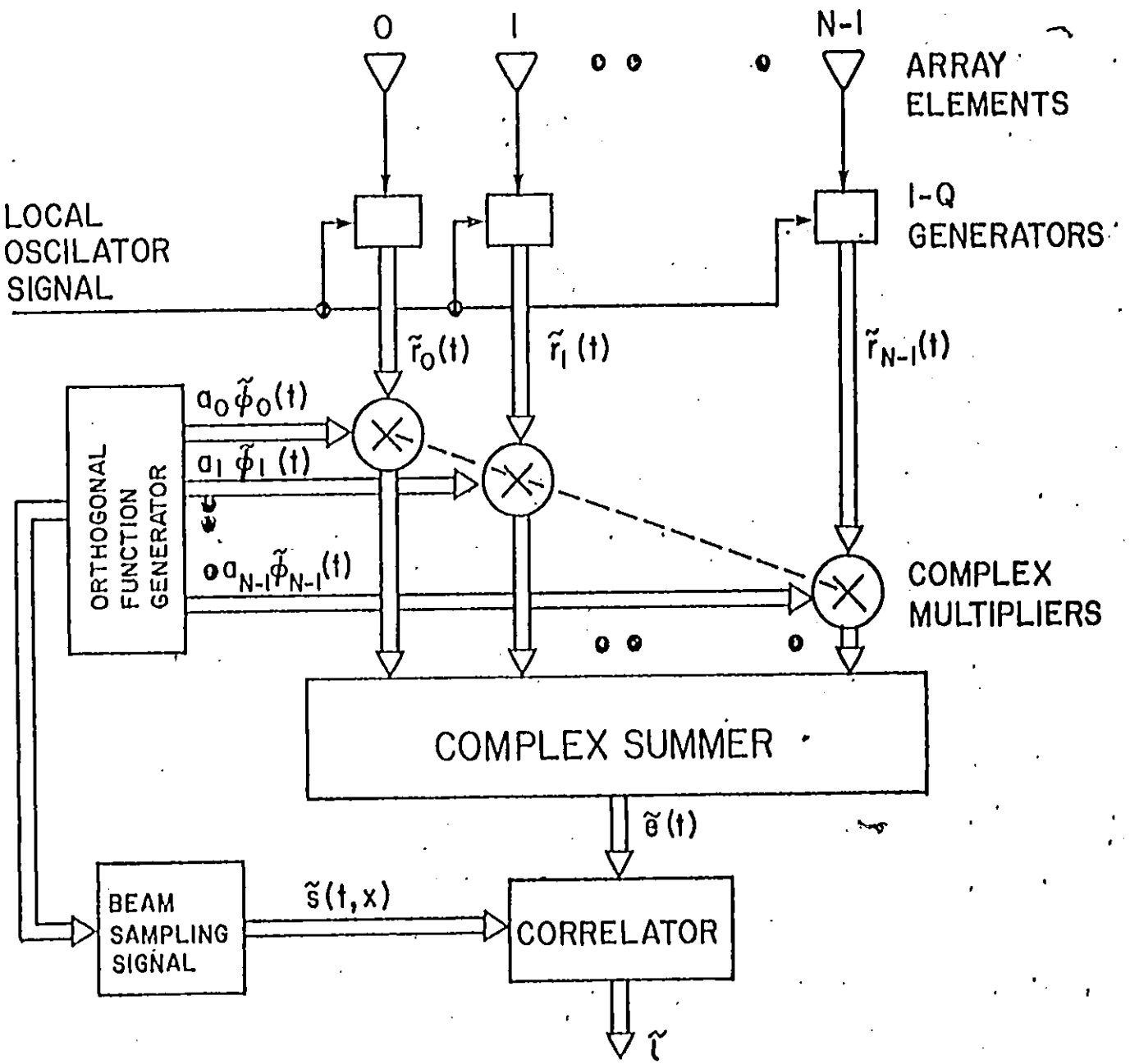

Fig. 2.8 Block diagram of time modulation scanning array

the received signal (on an element by element basis) simultaneously to a pair of multipliers. One multiplier is supplied with a local oscillator signal (which is synchronous with the RF source in the transmitter) and the other multiplier with the same oscillator signal except for a 90° phase-shift. The resulting multiplier outputs are then low-pass filtered, thereby yielding the in-phase (I) and quadrature (Q) components of the received signal, which provide a complex-valued representation of the signal. The set of operations, whereby the received signal at each element of the array antenna is defined in terms of its I- and Q-components, is represented in block diagramatic form by the I-Q generators in Fig. 2.8. The complex-valued output of each element is next multiplied (by means of a complex multiplier) by a corresponding component selected from a set of time-multiplexed (i.e., orthogonal) periodic trains of rectangular pulses. The contributions thus obtained from the various elements of the array are combined in a complex summer to produce a main beam that scans continuously with time at a rate equal to 1/T.

Consider a linear array consisting of N identical elements, assumed to have no mutual coupling between them. Let $\tilde{f}(t)$ denote the complex envelope of the transmitted signal. For a discussion of the complex representation of arbitrarily defined band-pass signals, see reference [16].

The complex envelope of the received signal at the pth element of the array, produced in response to a transmitted radar pulse, is given by (in the absence of noise):

$$\tilde{r}_p(t) = b \exp(jpx)\, \tilde{f}(t), \qquad p = 0, 1, \ldots, N-1 \quad (2.1)$$

where b = a complex-valued random variable which includes the combined effects of target cross-section and propagation-loss fluctuations

The quantity x in eq. (2.1) is related to the angle of target arrival θ (measured with respect to the normal to the line array) by

$$x = \frac{2\pi}{\lambda} d \sin \theta \quad (2.2)$$

where λ = the transmitted wavelength, and

d = element-to-element spacing of the array.

For a prescribed value of θ, the quantity x represents the phase-angle difference (in radians) measured between the signals received by any two adjacent elements of the array, assuming plane waves.

Figure 2.9 shows the signal-flow graph for the complete array processing system. The signal $\tilde{r}_p(t)$ at the pth element is multiplied by the corresponding function $a_p\tilde{\phi}_p(t)$ derived from a generator that produces a set of periodic trains of rectangular pulses that are orthogonal to each other. The coefficient a_p represents the amplitude weighting applied to the pth element; its value is

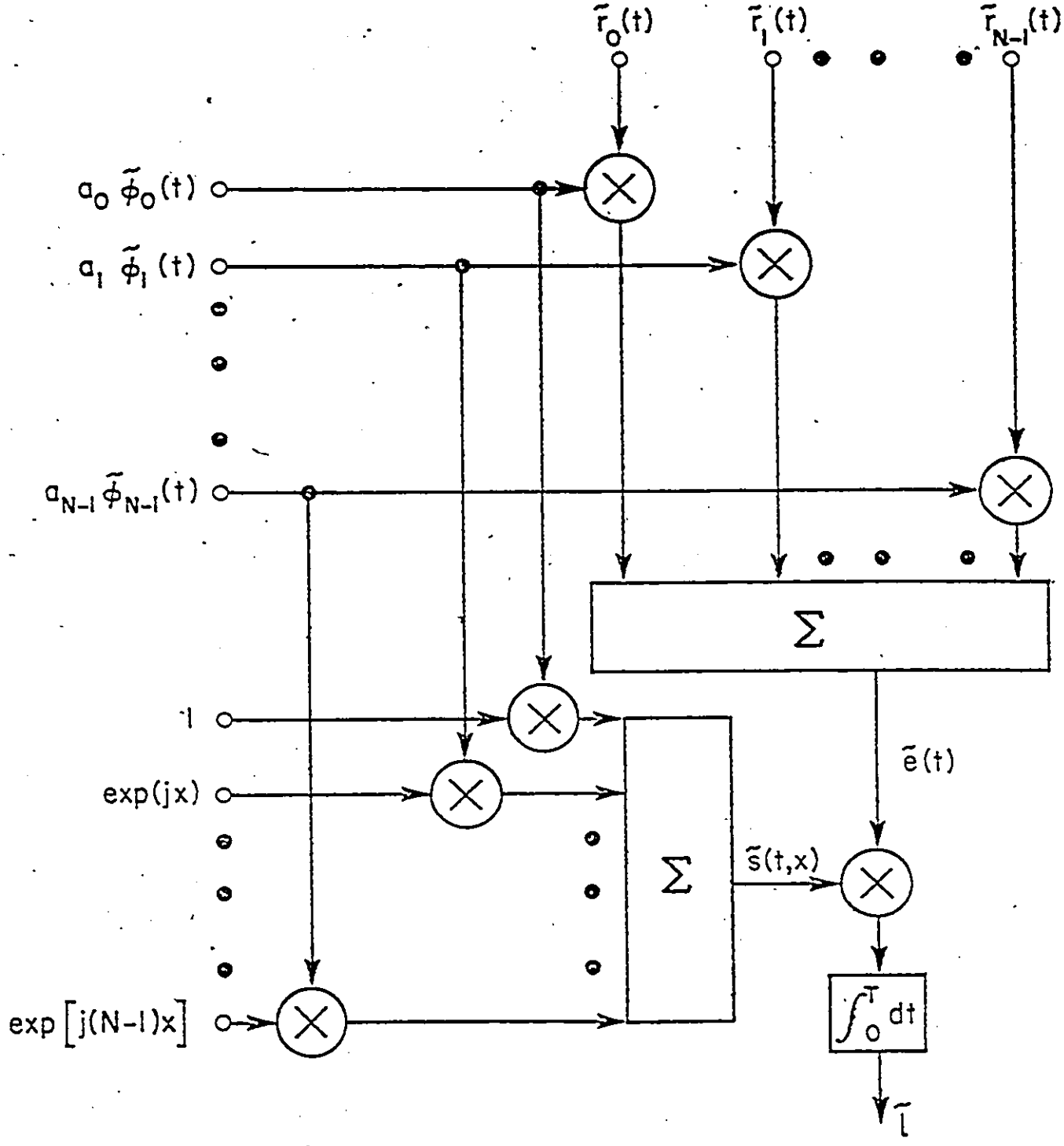

Fig. 2.9 Signal-flow graph for the complete signal processing of time modulation scanning array.

determined by the choice of a particular radiation pattern for the array. By summing the contributions of all the elements of the array obtained in this manner, we get

$$\tilde{e}(t) = \tilde{bf}(t)\ \tilde{s}(t,x) \tag{2.3}$$

where

$$\tilde{s}(t,x) = \sum_{p}^{N-1} a_p\ \tilde{\phi}_p(t)\ \exp(jpx) \tag{2.4}$$

The signal $\tilde{s}(t,x)$ of eqn. (2.4) is referred to as the beam-sampling signal for the following reason [8,17]. Suppose that it is required to steer the array in a look direction specified by the look angle θ or correspondingly the phase-angle difference x. From eq. (2.3) we see that this can be achieved by cross-correlating the summer output $\tilde{e}(t)$ with a beam-sampling signal $\tilde{s}(t,x)$. The result of this cross-correlation is defined by the variable

$$\tilde{z} = \int_0^T \tilde{e}(t)\tilde{s}^*(t,x)dt$$

$$= \int_0^T \tilde{bf}(t)\ \tilde{s}(t,x)\tilde{s}^*(t,x)dt \tag{2.5}$$

where T is the period of the periodic function $\tilde{\phi}_p(t)$, which is chosen equal to the transmitted pulse duration. In the case of a radar pulse with constant frequency f_c and constant amplitude k, we have

$$\tilde{f}(t) = \begin{cases} k, & 0 \le t \le T \\ 0, & \text{otherwise} \end{cases} \qquad (2.6)$$

We may therefore rewrite eq. (2.5) as

$$\tilde{\ell} = bk \int_0^T \tilde{s}(t,x)\tilde{s}^*(t,x)dt$$

$$= bk \int_0^T \sum_{p=0}^{N-1} \sum_{q=0}^{N-1} a_p a_q \tilde{\phi}_p(t) \tilde{\phi}_q^*(t) \exp(jpx)\exp(-jqx)dt$$

$$= bk \sum_{p=0}^{N-1} \sum_{q=0}^{N-1} a_p a_q \exp[jx(p-q)] \int_0^T \tilde{\phi}_p(t)\tilde{\phi}_q^*(t)dt \qquad (2.7)$$

Assuming that the set of orthogonal functions $\{\tilde{\phi}_p(t)\}$ are normalized, we have

$$\int_0^T \tilde{\phi}_p(t)\, \tilde{\phi}_q^*(t)\, dt = \begin{cases} 1, & p=q \\ 0, & p \neq q \end{cases} \qquad (2.8)$$

Hence, we may simplify eq. (2.7) as follows

$$\tilde{\ell} = bk \sum_{p=0}^{N-1} a_p^2 \qquad (2.9)$$

Suppose that the summer output $\tilde{e}(t)$ is cross-correlated with the beam sampling signal $\tilde{s}(t,x_o)$ for a specified value of x_o and that we are now interested in evaluating the response of the array viewed along a variable direction corresponding to x that is different from x_o. In

this case, we find that the cross-correlator output is a function of the deviation in the value of x from x_o, namely,

$$\Delta x = x - x_o$$
$$= \frac{2\pi d}{\lambda} (\sin\theta - \sin\theta_o) \qquad (2.10)$$

as shown by

$$\tilde{\ell}(\Delta x) = bk \sum_{p=0}^{N-1} a_p^2 \exp(jp\Delta x) \qquad (2.11)$$

When Δx is zero, this output assumes the value defined in eq. (2.9). Consider, for example, the case of a uniformly weighted array for which $a_p = 1$ for all p. Here we find from eq. (2.11) that the corresponding value of the cross-correlator output is

$$\tilde{\ell}(\Delta x) = bk \sum_{p=0}^{N-1} \exp(jp\Delta x)$$

$$= bk \exp\left[j\left(\frac{N-1}{2}\right) \Delta x\right] \frac{\sin\left(\frac{N}{2} \Delta x\right)}{\sin\left(\frac{1}{2} \Delta x\right)} \qquad (2.12)$$

which has the same form as the array pattern of a conventional uniformly weighted array antenna that uses phase shifters to achieve the required scanning.

We conclude therefore that by correlating the summer output $\tilde{e}(t)$ with an appropriate set of beam-sampling signals $\{\tilde{s}(t,x)\}$ corresponding to prescribed look directions (i.e., prescribed values of the quantity x), we are able to scan

the array into prescribed positions inside the visible region of interest.

It should be noted, however, that if the transmitted radar pulse involves a form of amplitude or frequency modulation or both, with the result that we can no longer assume the validity of eq. (2.6), then it becomes necessary to cross-correlate each elemental output of the array with a stored replica of the transmitted radar signal. This operation has to be performed before multiplication with the pertinent component derived from the orthogonal function-generator [17].

2.8 Summary

In a phased array, a number of antennas are interconnected to receive or radiate coherently. A beam can be formed and steered over a prescribed sector of interest by applying linearly progressive phase increments from element to element. There are a number of ways in which such progressive phase-sifts along the length of the array can be varied. This chapter has presented a brief description of different methods of scanning:

(1) Phase scanning: The radiation pattern of the array antenna may be steered to an angle θ by applying linearly progressive phase shifts from element to element, so that the phase between adjacent elements differs by $x = (2\pi/\lambda)\, d$

sin θ, where d is the inter-element spacing and λ is the operating wavelength. The phase-shifters, used for the above incremental phase shifts x, are electronically actuated to permit rapid scanning. It is dependent on frequency.

(2) Time-delay scanning: Dependence of the phase scanning on frequency is taken care of by using delay lines instead of phase shifters. This provides an incremental delay of $t = (d/c) \sin \theta$, where c is the velocity of propagation.

(3) Frequency scanning: A simple and effective method of scanning is to change the operating frequency in an antenna feed system composed of frequency sensitive phase shifters. The total phase shift through a fixed length of transmission line, which serves as a phase shifter, is $(2\pi f\ell/c)$.

(4) Multiple beam forming and switching: This involves the generation of a number of simultaneous beams and then selection of a particular one. Beam forming networks according to Blass [13] and Butler [14] are described briefly.

(5) Modulation scanning: One approach to beam scanning is to multiplex the element signals either in frequency or in time by using a technique known as modulation scanning which includes frequency modulation scanning and time modulation scanning as special cases.

CHAPTER 3

THE EXPERIMENTAL SYSTEM

3.1 Design Considerations of the Antenna

A Mills' cross array antenna, as previously mentioned, consists of two linear arrays at right angles to each other. Tucker [24] indicates that the total apertures of the two arms comprising the Mills' cross array antenna should be approximately equal for achieving maximum signal-to-noise ratio. Slattery [6] in his paper mentions that the array arms can be conveniently crossed at their centers resulting in a non-optimum system. He considers a Mills' cross array as consisting of 9 elements in each arm and finally he omitts the center elements of the two arms. This design, however, results in large side lobes because of the absence of the center element. To overcome this difficulty, we used, in our study, the Mills' cross array antenna of an even number of elements in each arm. The experimental system used consists of an 8 x 8 element array with the two arms of the array crossed at their centers. The array is designed to operate at X-band, so that an array of manageable physical dimension can be constructed. Each element of the array consists of an open-ended waveguide

horn that is fed by a matched coaxial cable. The gain of these horns is nominally 10 dB at midband. The beamwidth of these horns is approximately 50° for the above gain specification. The horns are placed 10 cm. apart in the array geometry resulting in a half power beamwidth of 2.3 degrees. The scanning is limited to 10 degree on each side of the normal to the array so as to avoid the appearance of grating lobes (which are 21.4° apart).

Measurement of the far field pattern of any aperture has always involved probing the field at a constant radius far enough away so that the aperture approximates a point source. Since the wave generated from the transmitting antenna is spherical, the phase front across the aperture of the receiving antenna will be plane only when the distance between the antennas is infinitely large and for any finite separation the phase front across the aperture will be curved. For the plane wavefront to be in error of 0.1 dB which is sufficiently accurate for most antenna work, the distance R between the antennas should be calculated according to the formula $R \geq 2A^2/\lambda$, where A is the aperture of the antenna and λ is the received wavelength. The symbol R, A and λ should be expressed in the same unit. The derivation of the above formula is given in Appendix A. The above expression results in a distance R = 35 meters for the antenna under study. Thus, the anechoic chamber with a

quiet zone of 8 x 8 x 2 meters can not accommodate the requirements for the desired antenna measurements in the Fraunhofer zone. In order to realize, with the quiet zone described above, a plane wavefront at the aperture of the receiving array, the structure is physically molded into a spherical surface having a radius of curvature less than or equal to $2A^2/\lambda$. Such a curved structure permits a plane wavefront across its aperture, the proof of which is given in Appendix B according to Bickmore [18]. Such measurements have less inherent phase error in the region of the main beam than the conventional measurements on a plane aperture at $2A^2/\lambda$. This follows the special focussing procedure described by Bickmore. It is apparent from Fig. 3.1 that the distance D by which the center of the array will be deflected is given by $D = (A/2) \cos \theta$. Also we have $\cos \theta = \sin (A/4R)$. Consequently, $D = A^2/8R$ is an excellent approximation to make the focussing as desired. With A = 80 cm and R = 8 meters, the ends of each arm of the Mills' cross array are thus deflected by 1 cm from their normal positions. The structure is pictured in Fig. 3.2 showing details of the receiving Mills' cross array along with the RF components used for baseband conversion.

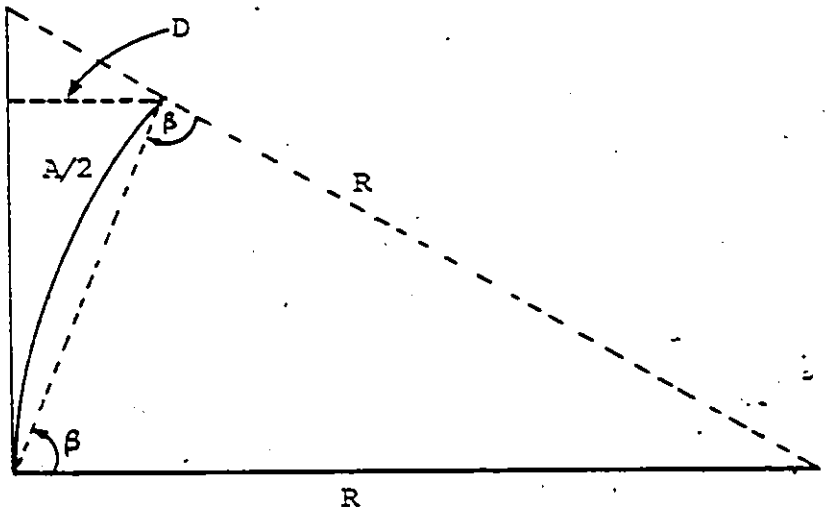

Fig. 3.1 Geometry of the curved array.

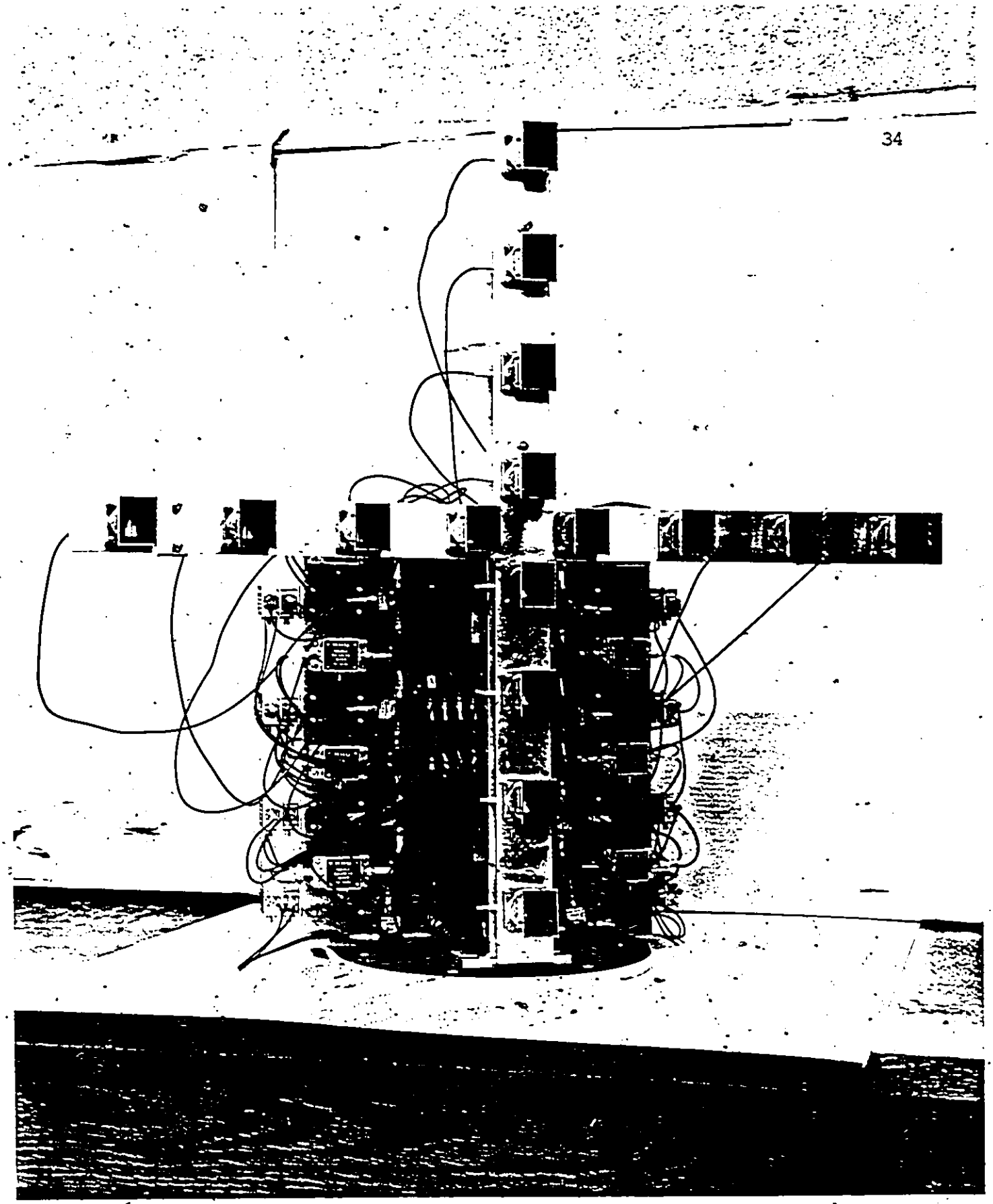

Fig. 3.2 Photograph of the receiving arrangement

3.2 Transmission of Microwave Energy

The transmitting antenna of the experimental system transmits a periodic train of rectangular pulses modulated onto a sinusoidal carrier wave of frequency 8.2 GHz. The carrier wave is obtained from a sweep oscillator HP-8620A, designed specifically for use with the Hewlett-Packard Model 8410A Network Analyzer system to provide a complete microwave measurement system. An external modulation signal of 1 KHz from a pulse generator HP-8008A is applied through EXT AM connector to modulate the output RF signal. The modulated signal is applied to the model HP-495A microwave amplifier input and taken at the output of the traveling-wave tube amplifier (TWTA). All voltages required by the TWTA are supplied by the regulated high voltage power supply and the modulator resident inside the microwave amplifier. It generates about 1 watt at the output with the application of 1 milliwatt or less at the input. The level of the output power can be set at any desired value. A portion of this microwave energy is transmitted by the transmitting horn and the rest is used to drive the mixers for baseband conversion. This division is done by using directional coupler right at the output of the microwave amplifier. The photograph of the transmitting horn along with the microwave amplifier is shown in Fig. 3.3. The microwave amplifier is placed conveniently near to the transmitting horn in the

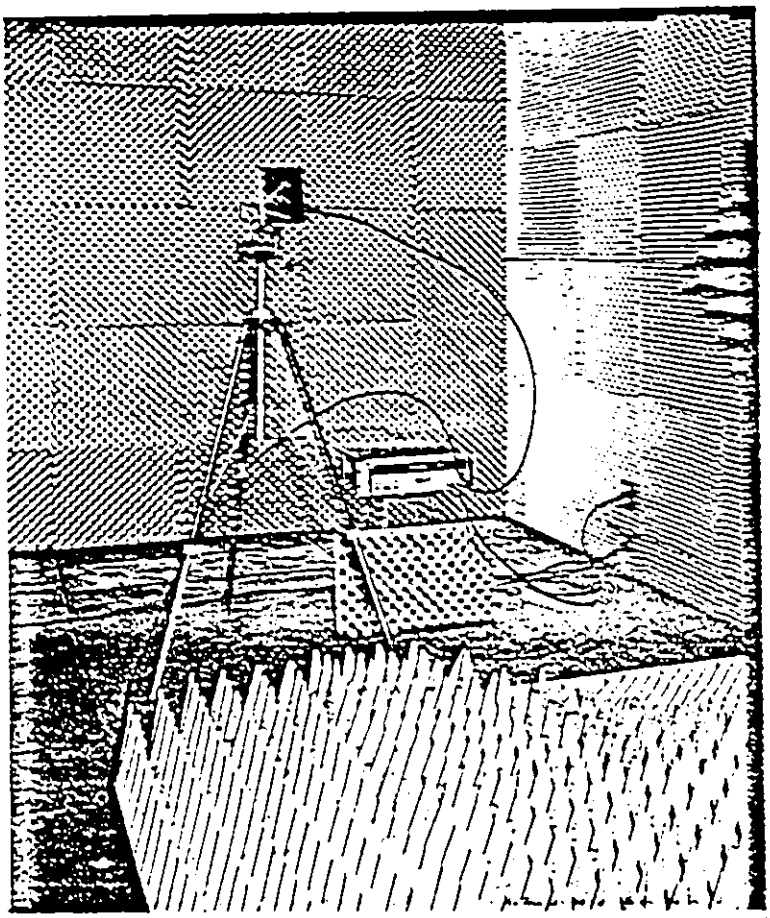

Fig. 3.3 Photograph of the transmitting arrangement.

anechoic chamber in order to avoid unnecessary attenuation in transmission lines.

It may be mentioned that the foam dielectric Heliax cable, used in transmission of energy at such high frequency from equipment to equipment, plays an important role in the experimental set-up. Those cables are ideal for use in phased-array radar applications or for connection of RF equipments. These cables offer low attenuation (0.2 dB/foot), complete RF shielding and flexibility compared to conventional solid dielectric cable of similar size. The photograph of the equipments used in measuring antenna response pattern is shown in Fig. 3.4. The sweep oscillator which is a member of the Network Analyzer is excluded in this figure.

3.3 The Baseband Processor

A possible implementation of digital hardware signal processor to scan the pencil beam over the prescribed sector using time-modulation scanning is achieved through the conversion of the RF signal into its baseband. This permits in shipping received signal outputs to signal processing unit without severe attenuation that may occur at x-band.

The RF signal received by each element of the array antenna is heterodyned to its baseband form (expressed in terms of in-phase and quadrature components) by using the

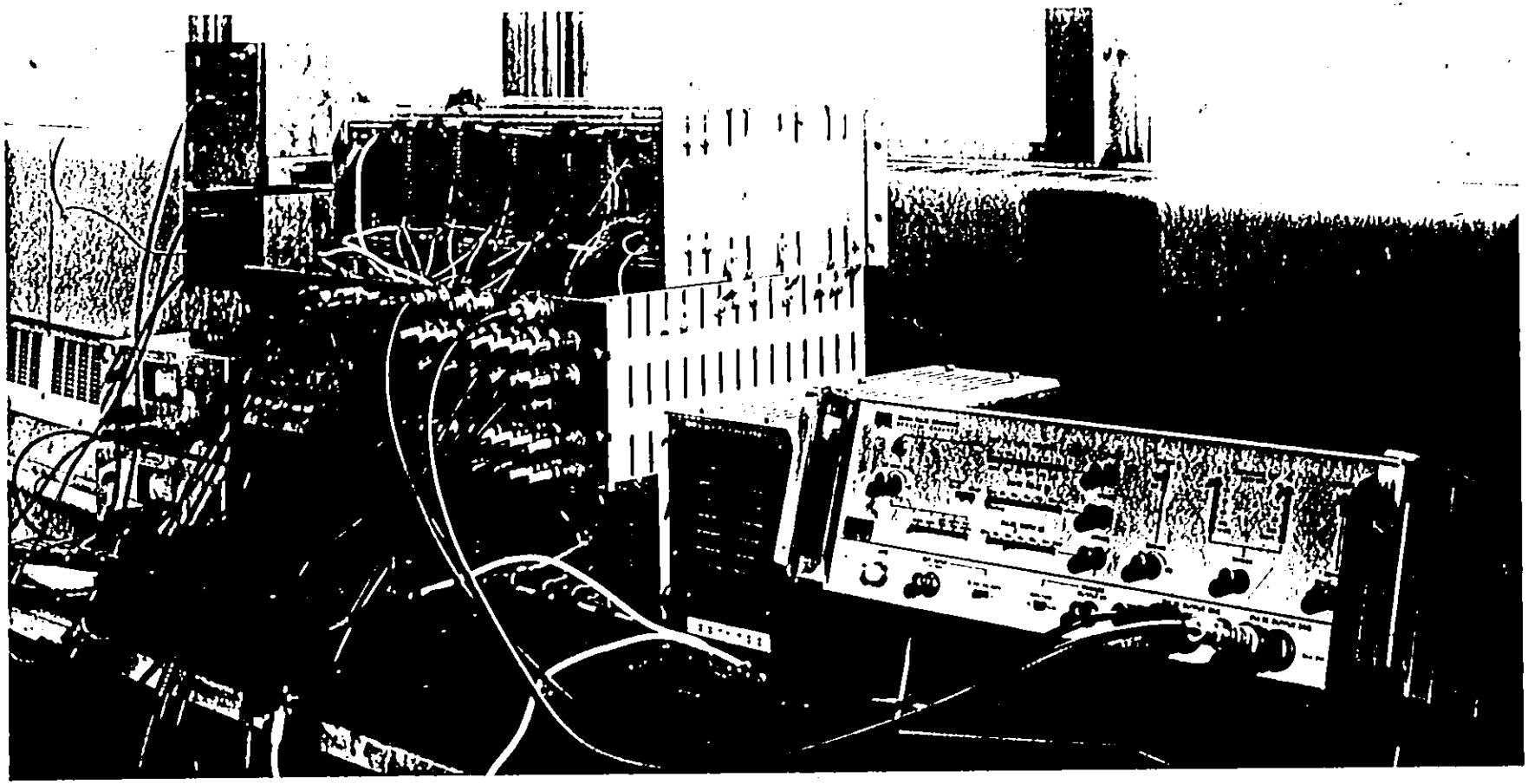

Fig. 3.4 Photograph of the equipments used in measuring the antenna response pattern

configuration shown in Fig. 3.5 for one arm of the array. This same heterodyning configuration is reproduced for the other arm of the array. This conversion into baseband form is required in order to make the implementation of the processor using digital hardware possible. Specifically, the signal received by each element is applied, through a two-way power divider, to a pair of mixers which are supplied with two sinusoidal waves in quadrature with each other. The 90° phase-shift required for this mixing process is obtained by means of a line stretcher, as indicated in Fig. 3.5.

The mixer outputs are next applied to a baseband processor which uses within-pulse scanning in order to avoid the loss of received power, and also to provide a high data rate capability [7]. Scanning over the sector of interest is achieved by sweeping the individual fan beams, produced by the two arms of the array, at different speeds so that the pencil beam at their intersection point moves across the sector in a raster-like fashion. Denoting the number of raster lines by M and the duration of the transmitted radar pulse by T, one arm of the array is scanned at a rate equal to 1/T and the other is scanned at a faster rate equal to M/T. Thus, the desired aperture excitation is achieved by progressively switching on each element of the slow arm of the array for a duration equal to T/N seconds and then

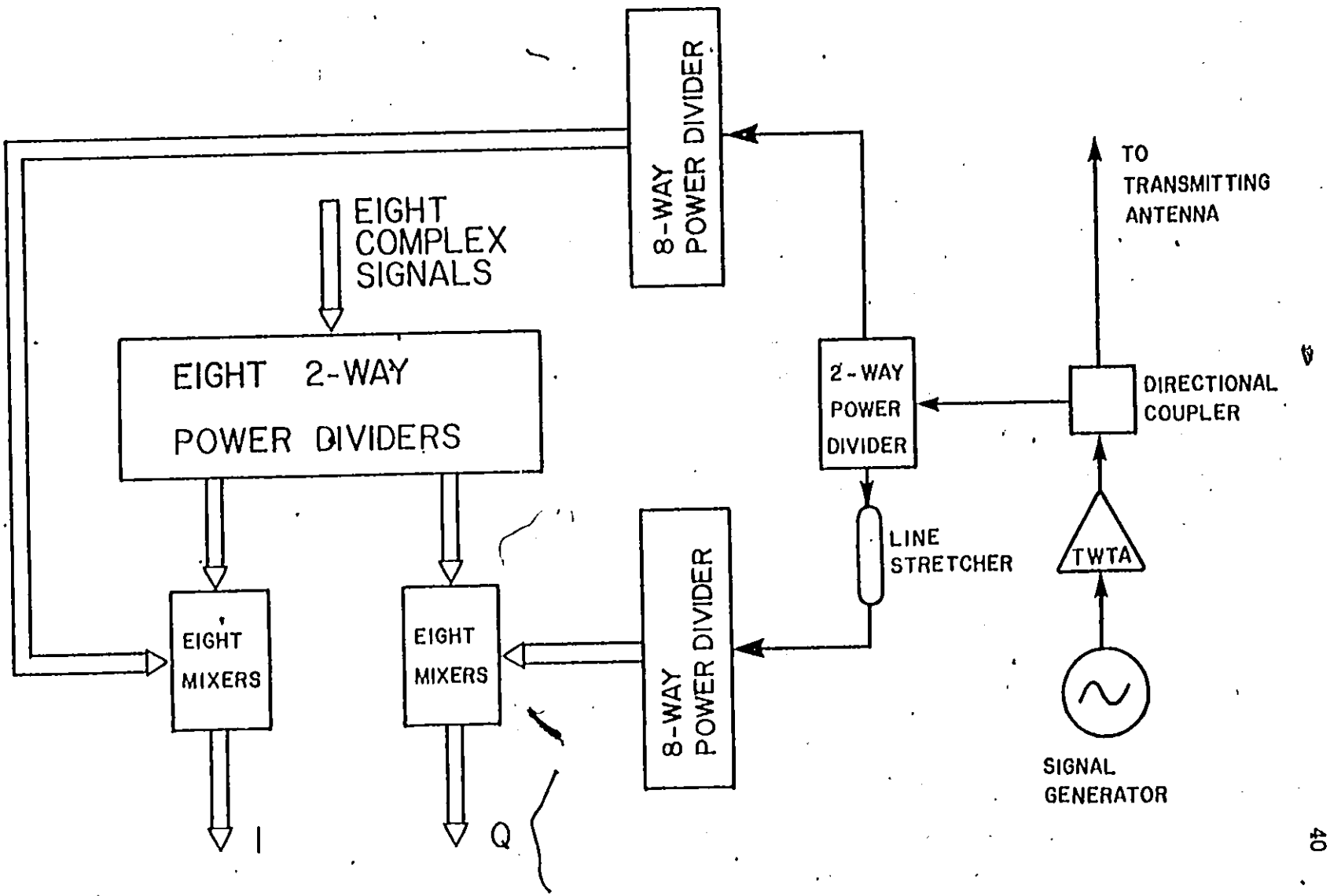

Fig. 3.5 Schematic diagram illustrating the baseband conversion.

switching it off for the rest of the period, whereas each element of the fast arm is progressively switched on for a duration equal to T/MN seconds in a synchronous manner with the slow arm. The N denotes the number of elements in each arm of the array.

A block diagram of the baseband processor is shown in Fig. 3.6. This processor is implemented using digital hardware, for which time modulation scanning [9] is rather well-suited. The switching operations on the mixer outputs are performed by means of 4 multiplexer switches, with one pair operating on the in-phase and quadrature components of the baseband signal derived from one arm of the array, and the other pair operating on the in-phase and quadrature components of the baseband signal derived from the second arm of the array. The time-multiplexed signals obtained from the multiplexer switches are low-pass filtered, amplified, and then applied to a corresponding set of analog-to-digital (A/D) converters. The required data in digital form is now available for further processing.

Suppose that it is required to steer the array in a look direction specified by the angle θ_1, measured with respect to the normal to the slow arm, and the angle θ_2, measured with respect to the normal to the fast arm. To achieve this, the time-multiplexed signals obtained from the two arms of the array, after analog-to-digital (A/D)

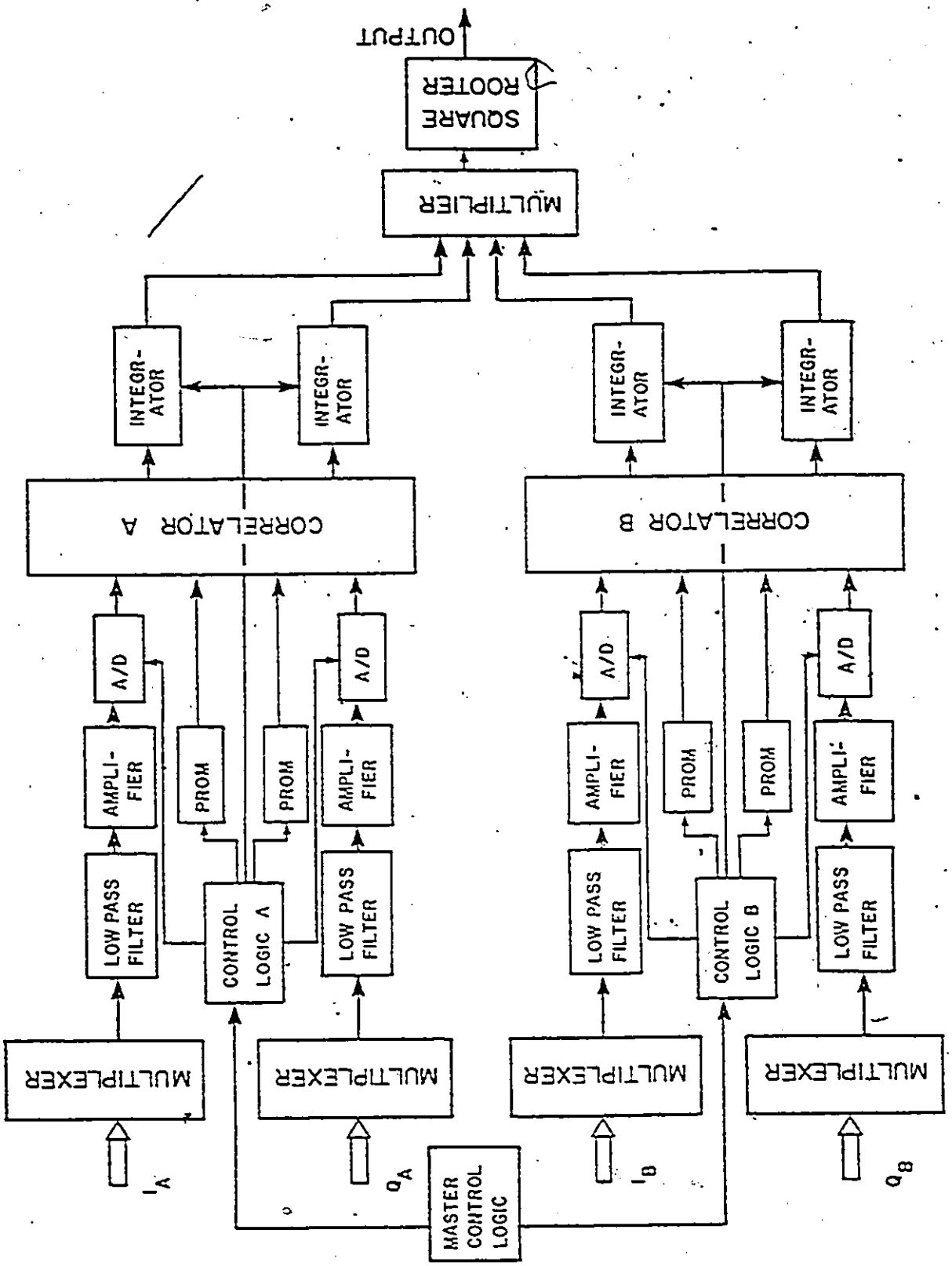

Fig. 3.6 Complete block diagram for baseband processor used in the Mills' cross array.

conversion, are respectively correlated with the beam-sampling signals $s(t,x_1)$ and $s(t,x_2)$ which, for pre-selected values of x_1 and x_2, are stored in the form of look-up tables in programmable read-only memories (PROM). The variables x_1 and x_2 correspond to the angles θ_1 and θ_2, respectively, according to eq. (2.2). The resulting complex-valued outputs of these 2 correlators are properly scaled and then multiplied together to produce a complex signal representation of the prescribed pencil beam. The photographs of the front view and rear-view of the digital baseband processor are shown in Figs. 3.7 and 3.8 respectively.

3.3.1 Control Circuitry

The scheme uses within-pulse scanning to obtain information about all targets in the prescribed scanning sector. This is achieved by appropriate control of the clock pulse at different stages of the digital baseband processor. The control circuitry provides all necessary clock pulses and control signals for the baseband processor. For synchronous operation of the whole system, it is necessary that the clock pulses and the pulse train for modulating the RF signal in the sweep oscillator be obtained from the same source. The modulating periodic pulse train is obtained by means of appropriate frequency divider. The

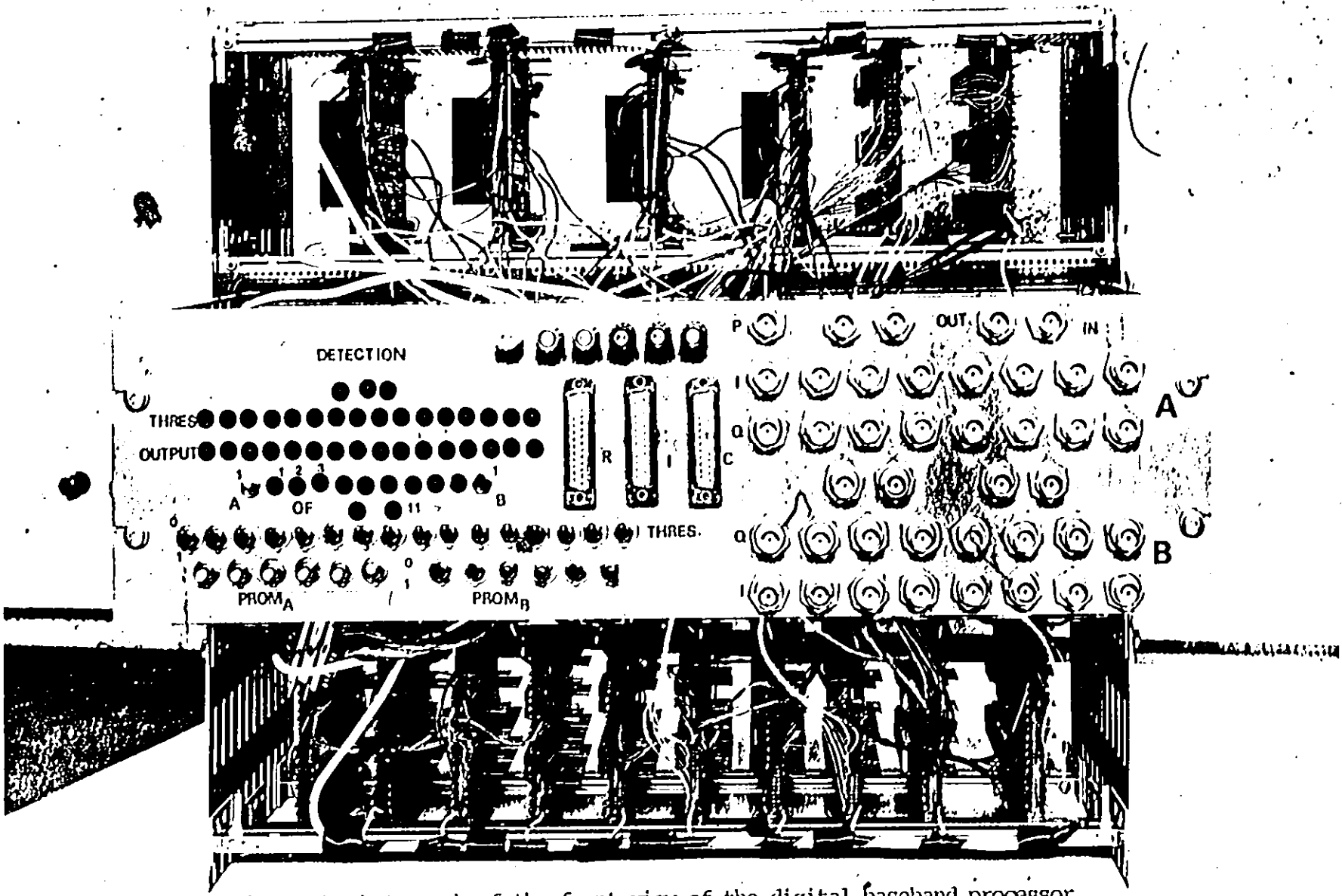

Fig. 3.7 Photograph of the front-view of the digital baseband processor

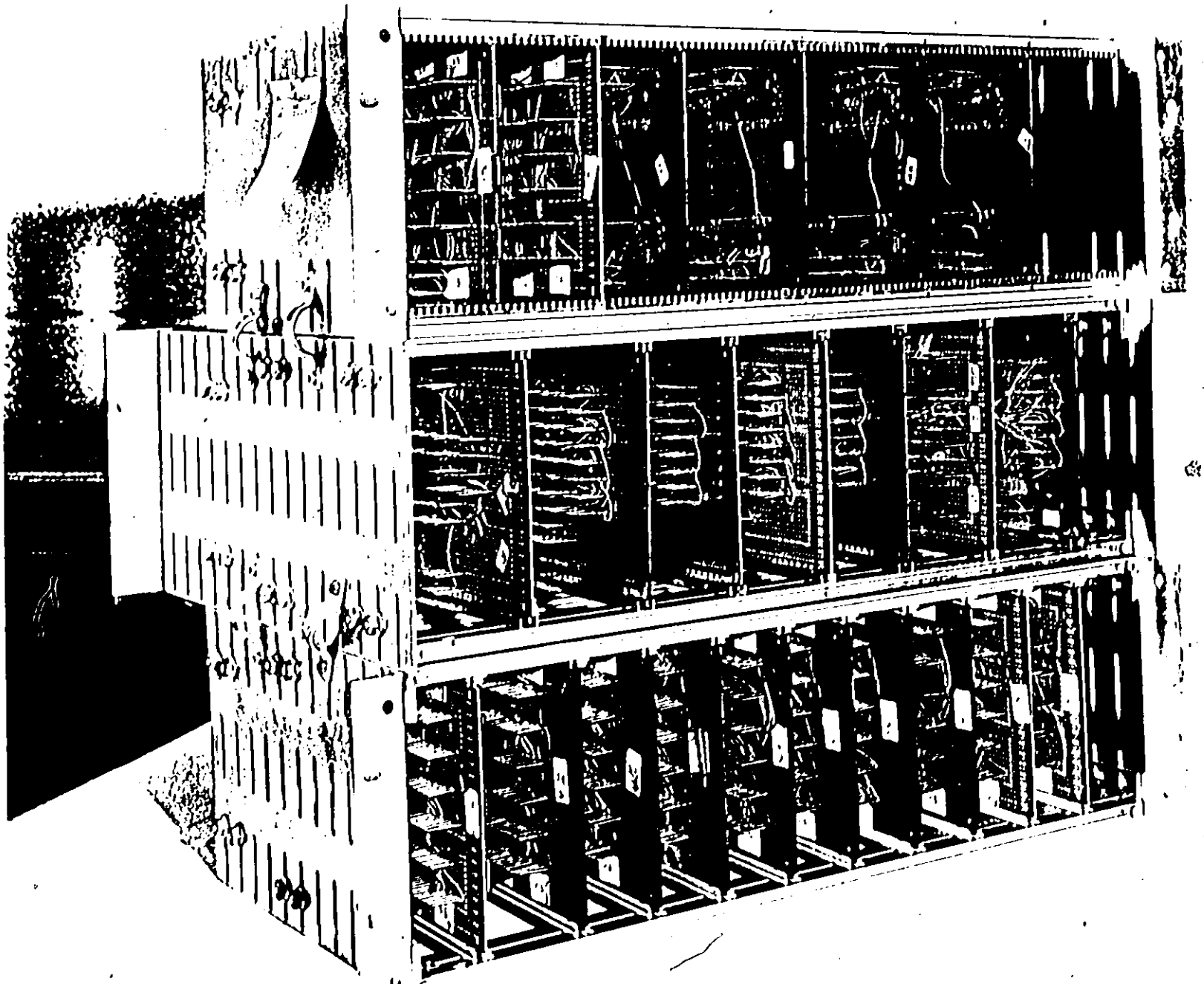

Fig. 3.8 Photograph of the rear-view of the digital baseband processor

address counters for the multiplexer switches and programmable read-only memories, convert commands for the analog-to-digital converters, clock pulses for the registers in the integrator units and load signals for the counters associated with different units, are obtained from the master clock pulse with appropriate delays. Since each circuit of the digital baseband processor has its own time delay to complete its operation, time delays at different stages will be different. In order to make synchronous operation of the system possible, the desired time delays for different stages are obtained from monostable multivibrators 74123 by incorporating external capacitors and resistors of appropriate values. The monostables provide flexibility in controlling the pulse width of the clock pulse, either to lengthen the pulse by retriggering or shorten by clearing. Delays of the order of 10 ns are obtained by using simple inverter gates.

3.3.2 Analog-to-digital Conversion of the Time-multiplexed Signal

The baseband analog data is acquired in digital form in order to make the desired signal processing operations possible. To digitize data from different analog channels, a time-sharing process is introduced. The input of a single A/D converter is time-multiplexed in sequence among the

various element signals. In the system configuration we have used 4 A/D converters. An additional logic circuit keeps track of which data source is coupled to the converter at any instant as shown in Fig. 3.9. The multiplexing operation is done by employing the unit Am 3705 which is a MOS monolithic 8-channel multiplexer switch with an output-enable control and one-out-of-eight decoder. It has a switching time of 1 μs which is appropriate for our study. The time-multiplexed signal is then applied to the low pass filter to remove unwanted components of the input signal. The filtered signal is then scaled up from millivolt level to the A/D converter's full scale input level. An operational amplifier with appropriate closed loop gain is used for this purpose. The analog signal is thus appropriately conditioned to be ready for digital conversion. Upon receipt of the external convert command from the control circuitry, the previous data sample from each A/D converter is cleared from the output registers. Each bit is then successively compared against the amplitude of the input signal and is held as "0" or turned on as "1" until all bits have been tried. The parallel data output is not available for transfer for further processing until its status output changes from logic "1" to logic "0". Bipolar 2's complement is obtained by using the complement of the most significant bit (MSB). The required data in digital

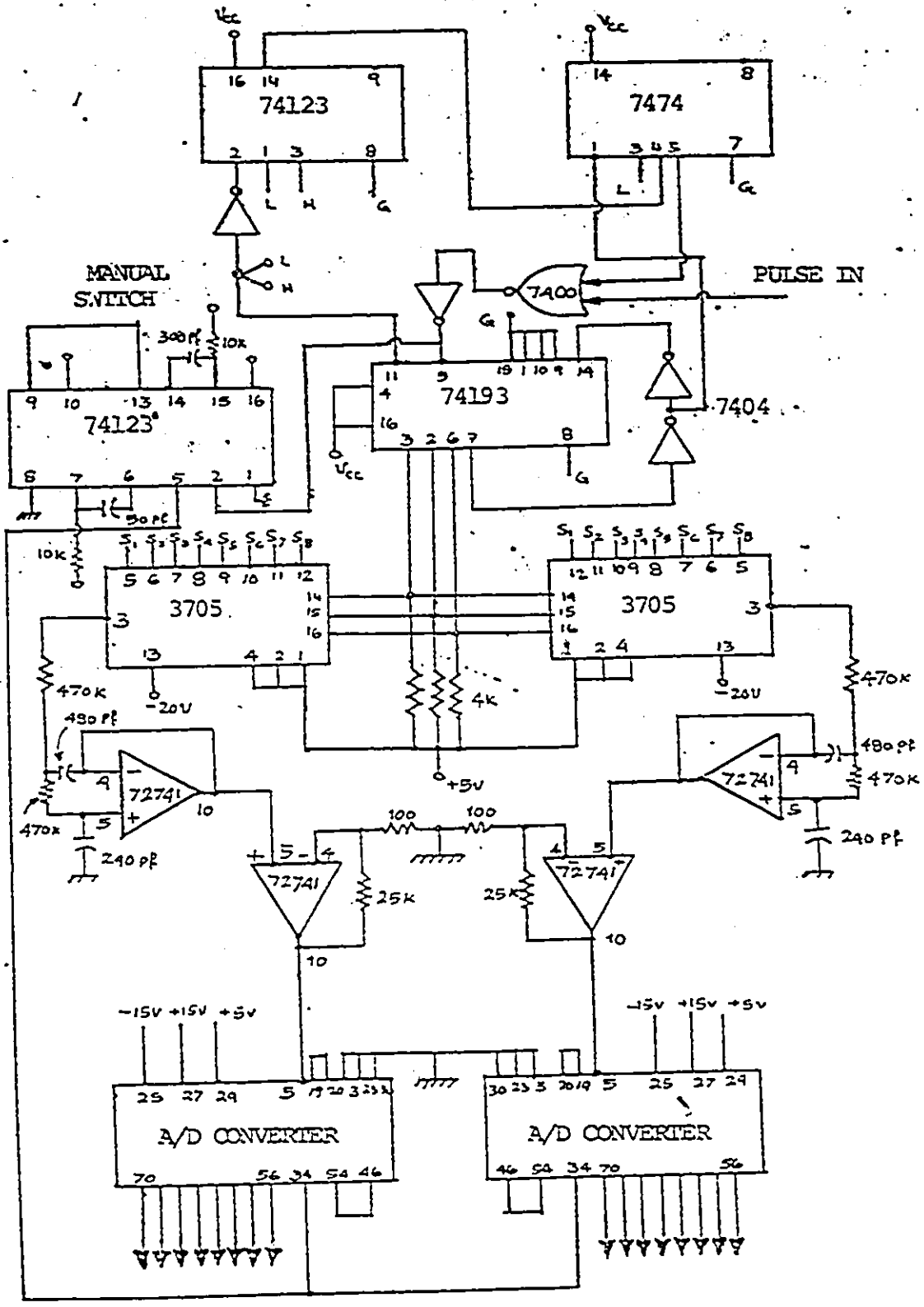

Fig. 3.9 Detailed control circuitry illustrating the operation of analog-to-digital converters.

form is now available for further processing. The circuit diagram involved in this process of analog-to-digital conversion is given in Figure 3.9 which describes the operation of one arm. The other arm has the same circuitry except for the timing control.

3.3.3 Generation of the Beam Sampling Signal

The time-multiplexed signal, after analog-to-digital conversion, is correlated with a beam sampling signal to steer the array pencil beam to a desired look direction. The beam sampling signal for a pre-selected look direction in 2's complement notations is stored in the form of a look-up table in a programmable read-only memory (PROM). The Am 1702 used for the above purpose is a 256-word by 8-bit field programmable MOS read-only memory. This unit is designed to have all outputs at logic HIGH level. Each bit in the memroy can be electrically programmed to a LOW-level. The Am 1702 can be erased by controlled exposure to ultra-violet light. After it is erased, the Am 1702 can be reprogrammed by the PROM programmer, each word being located by the corresponding address. Thus it provides the flexibility of applying different types of aperture distribution in order to modify the side lobe structure of the response pattern.

The 8-bit address to the PROM is obtained through two counters, 74193, connected in cascade as shown in Fig. 3.10.

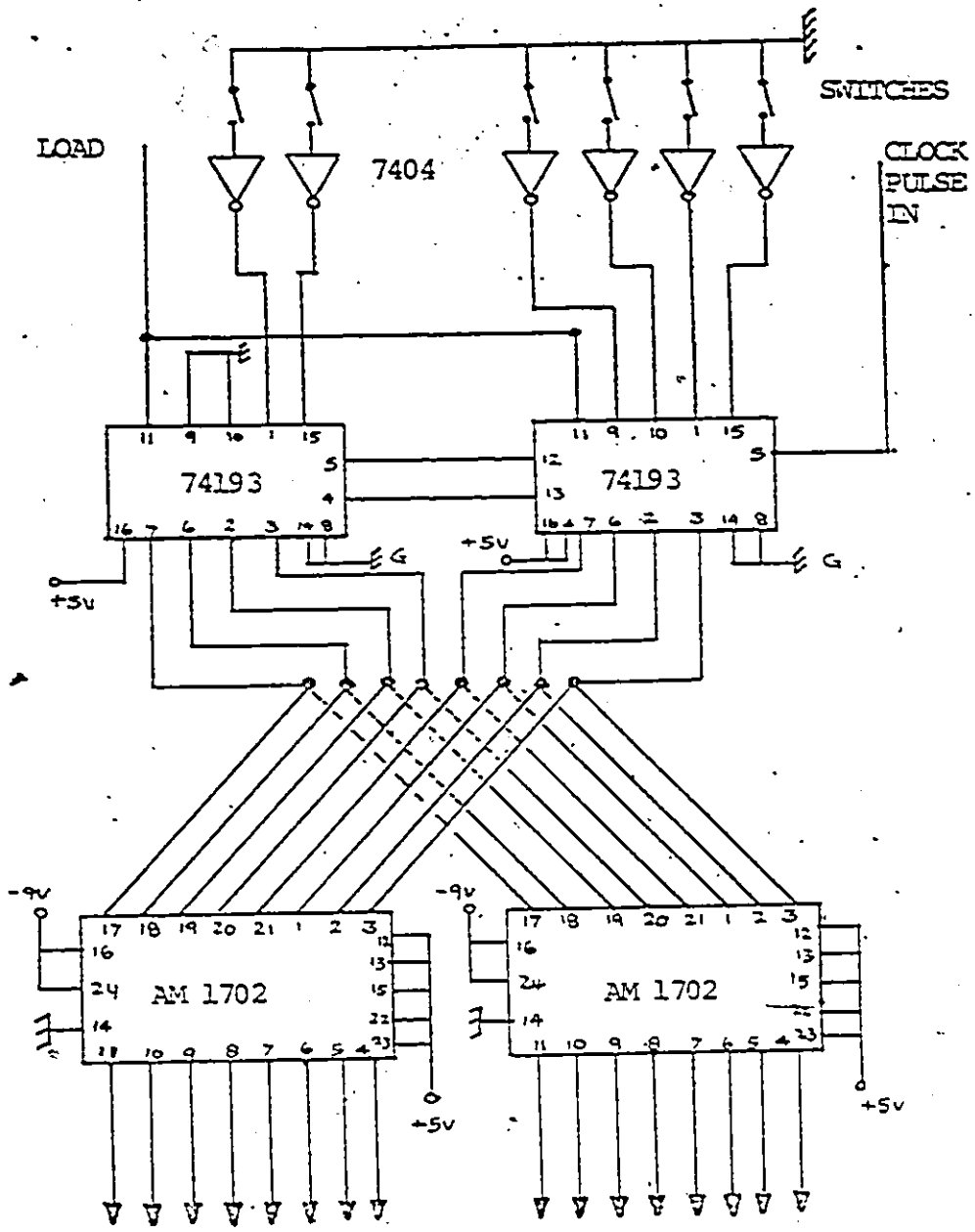

Fig. 3.10 Detailed circuit diagram for the generation of beam sampling signal.

Manual switches along with inverter gates are used on the input side of the counter unit to provide the beam switching facility. A particular beam is selected by setting the manual switches to appropriate positions so that they collectively represent the first address corresponding to that beam. The counter unit with the manual switches set at appropriate positions, provides the PROM with 8 address sequencially required for a particular beam position.

3.3.4 Correlation and Integration

The operation of cross-correlation involves multiplying the time-multiplexed output by the complex conjugate of the beam sampling signal which is resident in the PROM. Thus it includes the arithmetic operations of multiplication, addition and subtraction. Multiplication is performed by using Am 2505. It is a high speed digital multiplier that can multiply numbers represented in 2's complement notation and produce a 2's complement product without correction. The device consists of 4 x 2 multipliers that can be connected to form iterative arrays capable of multiplying numbers. The device assumes that the most significant bit in a word carries a negative weight and therefore can be used in arrays where its multiplicand and multiplier have different word lengths. Figure 3.11 illustrates the connection scheme of 8 x 8 bit 2's

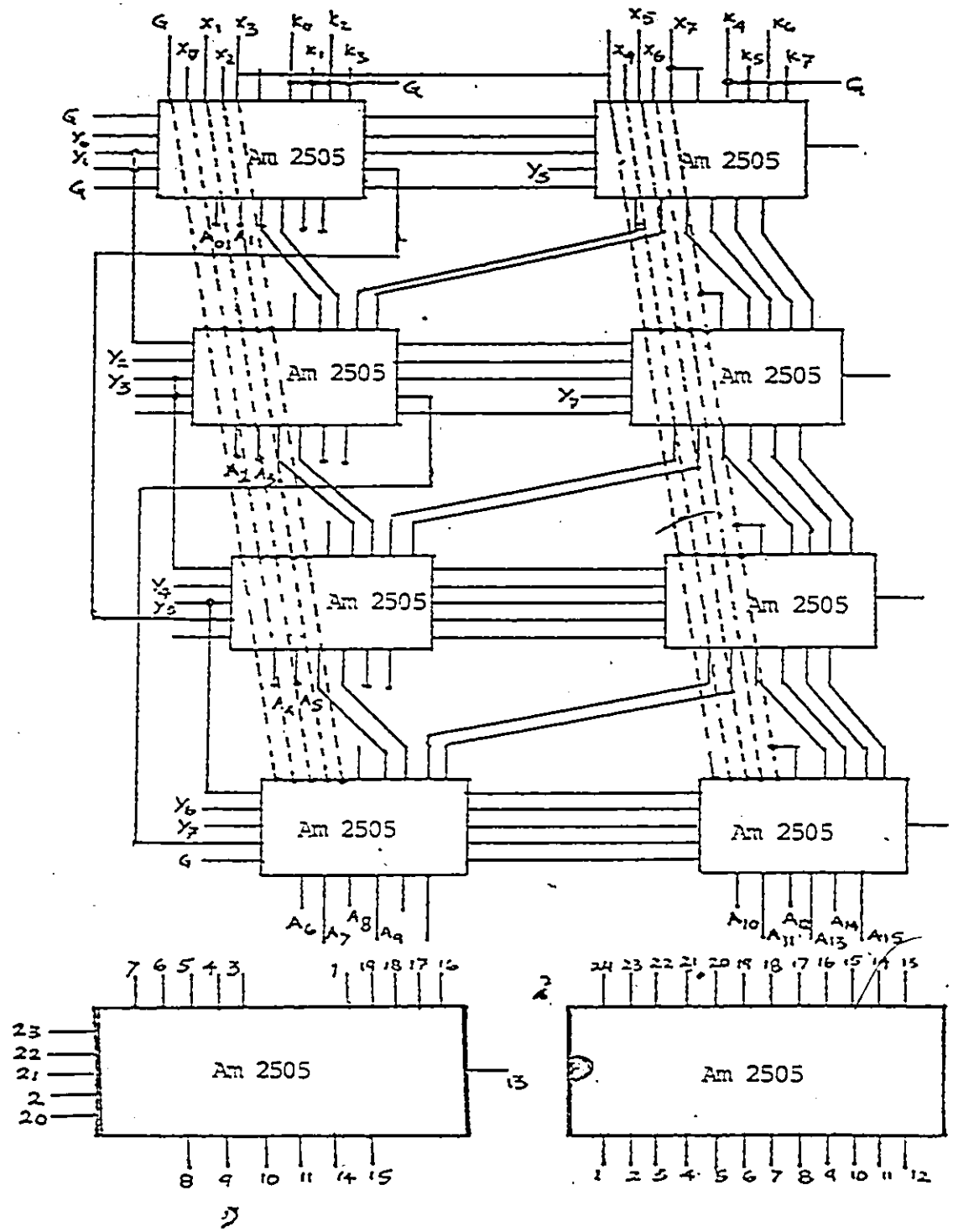

Fig. 3.11 Connection scheme of 8X8 bit 2's complement multiplication employing Am 2505 as a building block.

complement multiplication. The device provides a 16-bit word at its output pins.

The 16-bit word outputs of the multiplier units are appropriately added and subtracted for desired cross-correlation. The 74283, which is a 4-bit binary full adder, is used for both arithemetic operations. The 16-bit adder and subtracter are obtained by cascading four 4-bit binary adders. The typical add and subtract time is 43 nanoseconds for two 16-bit words. The integration necessary to improve the detectibility is conveniently done after correlation. The operation of integration involves the use of adder units and two shift register units. Each of the shift register units are supplied with different clock pulses, one of which has 8 times pulse repetition rate. The operation of integration is illustrated by the block schematic diagram shown in Fig. 3.12. The double lines in the figure indicate transmission of 16-bit words.

The complex valued outputs of the two correlators, after appropriate integration, are properly multiplied together to produce a complex representation of the prescribed pencil beam.

3.4 Summary

In Chapter 3, we have described the Mills' cross antenna that has been constructed for the experimental

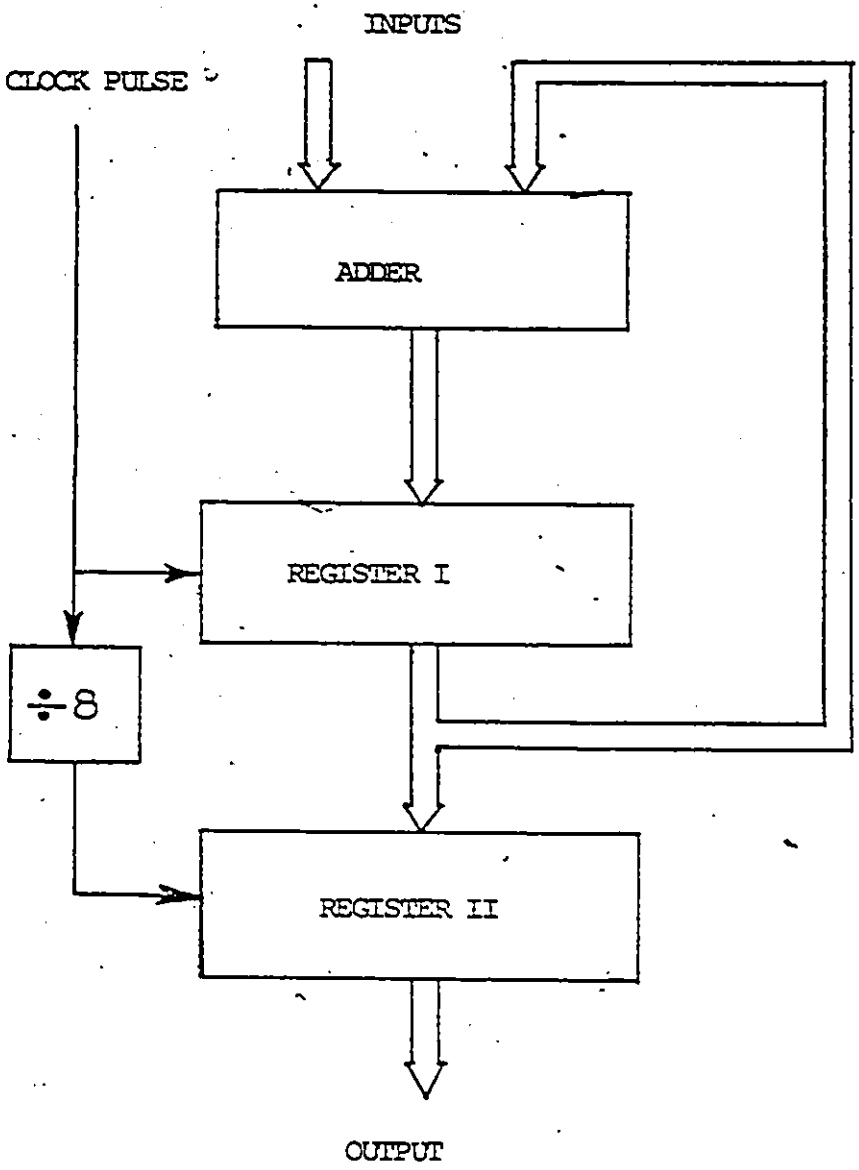

Fig. 3.12 Block schematic diagram illustrating the operation of integration. Double lines indicate the transmission of 16-bit words.

system. The experimental system employed, consists of an 8 x 8 element array with the two arms crossed at their centers. The array is designed to operate at x-band, so that an array of manageable physical dimension can be constructed. The horns forming the Mills' cross are spaced 10 cm. apart in each arm resulting in a half power beamwidth of 2.3 degrees. The scanning is limited to 10 degrees on each side so as to avoid the appearance of grating lobes. In order to make measurements possible in the anechoic chamber, the structure is physically molded into a spherical surface having a radius of curvature less than or equal to $2A^2/\lambda$, where A is the aperture and λ is the operating wavelength.

In the second part of this chapter, the digital base-band processor implementing the time modulation technique for the desired raster-like scanning is described. The RF signal received by each element is heterodyned to its base-band form. The scheme uses within-pulse scanning to have simultaneous information about all targets in the prescribed sector. Synchronous operation of the whole system is achieved by deriving all necessary clock pulses and controls from the master clock pulse.

The analog-to-digital (A/D) converters are time-shared by using a multiplexer switch for each A/D converter. The processor offers the flexibility of applying different

types of aperture distribution in order to modify the side-lobe structure of the response pattern. This is obtained by merely changing the look-up tables stored in the programmable read-only memories (PROM). The cross-correlation involved in the baseband processor includes the operations of multiplication, addition and subtraction. All arithmetic operations are done in 2's complement notations to take care of negative numbers. The integration necessary to improve the system performance is conveniently done after correlation.

CHAPTER 4

EXPERIMENTAL RESULTS AND DISCUSSIONS

4.1 General

The Mills' cross array, that has been designed and built to test and verify the idea of time modulation scanning using digital baseband processor, consists of waveguide horns as its elements. The horns are spaced 10 cm apart, the restriction being imposed because of the array geometry and dimensions of the horns, resulting in a half-power beamwidth of 2.30°. The antenna thus constructed has a visible region that is defined by $\pm 10^{\circ}$ in both horizontal and vertical directions of scanning with respect to boresight of the array, as illustrated in Fig. 4.1. Uniform scanning over all parts of the sector is best achieved by sweeping the individual array beams so that the crossing point moves across in sector in a raster-like fashion. The parameters of the experimental system are as follws:

Number of radiating elements (in each arm) = N = 8

Number of raster lines = M = 5

Duration of the transmitted pulse = T = 500 μs

The number of raster lines is determined by the beamwidth and the angle of the visible region.

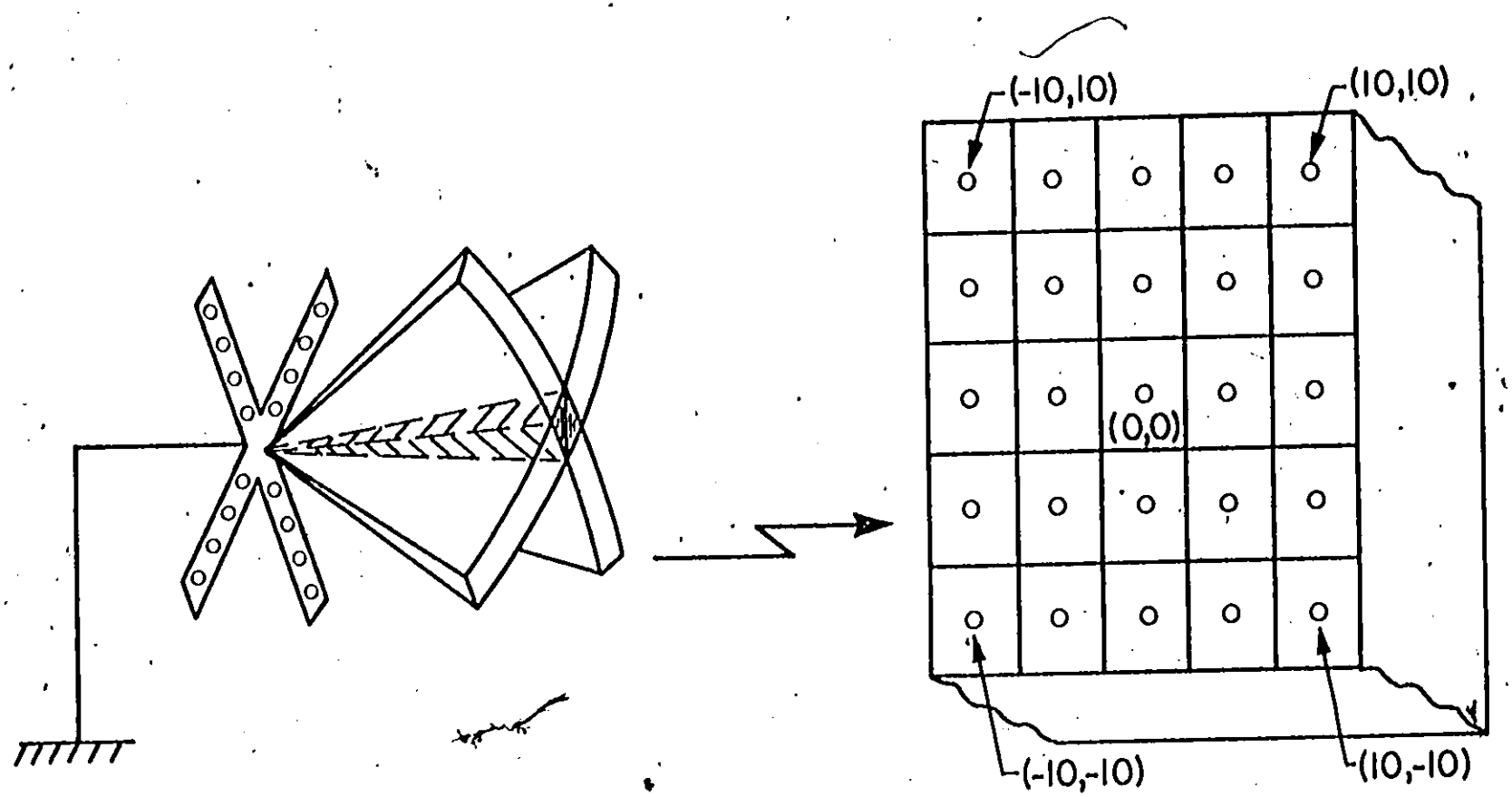

Fig. 4.1 The Fan beams along with the prescribed scanning sector for the Mills' cross array.

The response patterns of this experimental array (used as a receiver) are measured as follows. The array is mounted on an antenna positioner located at one end of an anechoic chamber, with a transmitting horn located in a fixed position at the other end of the chamber. The antenna positioner is rotated into different positions so as to provide different look directions for the array. The antenna patterns are thus measured at six different angular positions for one quadrant of the scanning sector. Because of symmetry of the system, similar results would be obtained for the other three quadrants of the scanning sector.

In this chapter, we present the results [19] of a number of response patterns of the Mills' cross array antenna to targets at different positions in one quadrant of the prescribed sector. The response patterns are taken for both uniform and Chebyshev distributions. This is a matter of simply changing the look-up table of the programmable read-only memory. The other methods of aperture illumination could also be easily applied to achieve desired pattern structures. For target at any one position in the prescribed sector, the strengths of the signals at all 25 different discrete positions are recorded from the output of the digital baseband processor unit. The digital outputs available in 16 bits are then presented in the form of a three dimensional surface projected on a two dimensional

plane employing a digital plotting system in the CDC 6400 computer. This is obtained from the measured discrete data by interpolating between the known values using the method of cubic spline [20]. This proves to be an effective tool in the elementary process of interpolation. Since the spline funtions constitute a relatively vast new subject in analysis, a very short description is given in Appendix C to define the method of cubic spline. The response patterns for other target positions in the quadrant of interest are obtained exactly in the same way. In all patterns, the main lobe has its peak value normalized to 0 dB. Also, the sidelobe level in any region of interest is obtained by constructing a plane parallel to the (θ_1, θ_2) plane of the figure and through the peak point of sidelobe level in question; the intersection of this plane with the vertical axis yields the required sidelobe level in dB.

4.2 Uniformly Weighted Array

The Mills' cross array, as previously mentioned, consists of two linear arrays arranged at right angles. The array is named according to the type of aperture illumination applied to each arm of the array. The Mills' cross array is said to be uniformly weighted array if all the elements in each arm are uniformly weighted. A uniform distribution in the aperture yields maximum directivity.

This form of weighting produces a half-power beamwidth equal to $(0.88\ \lambda/A)\cos\theta$, where λ is the operating wavelength, A is the aperture length and θ is the angle of the look direction measured with respect to the normal to the array geometry (for details see Appendix D). The highest side lobe level is 13.5 dB below that of the main lobe. By virtue of the fact that the 2 arms of the array are at right angles, we find that the half-power beamwidth and highest sidelobe level for a Mills' cross array have the same values as the corresponding ones for either arm. Figures 4.2 to 4.7 represent the three-dimensional plots of the response patterns for 6 different look directions in order to indicate the scanning capability of the Mills' cross array along the prescribed sector. In Table 4.1, we have summarized the half-power beamwidth (in degrees) and the highest side lobe level (in dB) for the above response patterns, based on theory and measured results. Note that the main lobe has its peak normalized to 0 dB.

4.3 Chebyshev Weighted Array

As is well-known, the high sidelobe level of a uniformly weighted array can be reduced, at the expense of increased half-power beamwidth, by applying some form of nonuniform weighting to the individual elements of the array [21]. For example, by exciting the elements of the array so

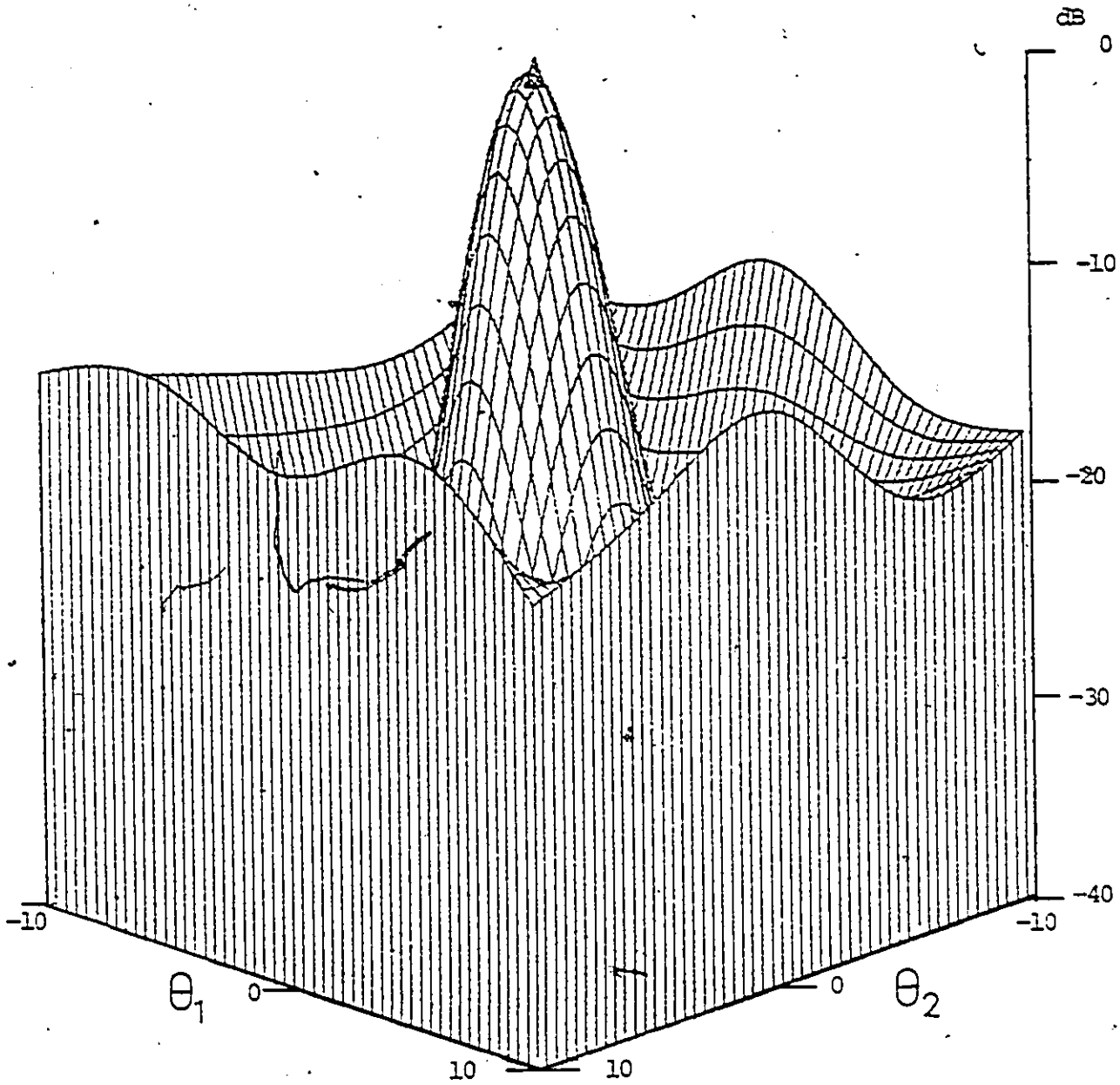

Fig. 4.2 Response pattern of the Mills' cross array antenna for the uniform aperture distribution when the target is at (0,0).

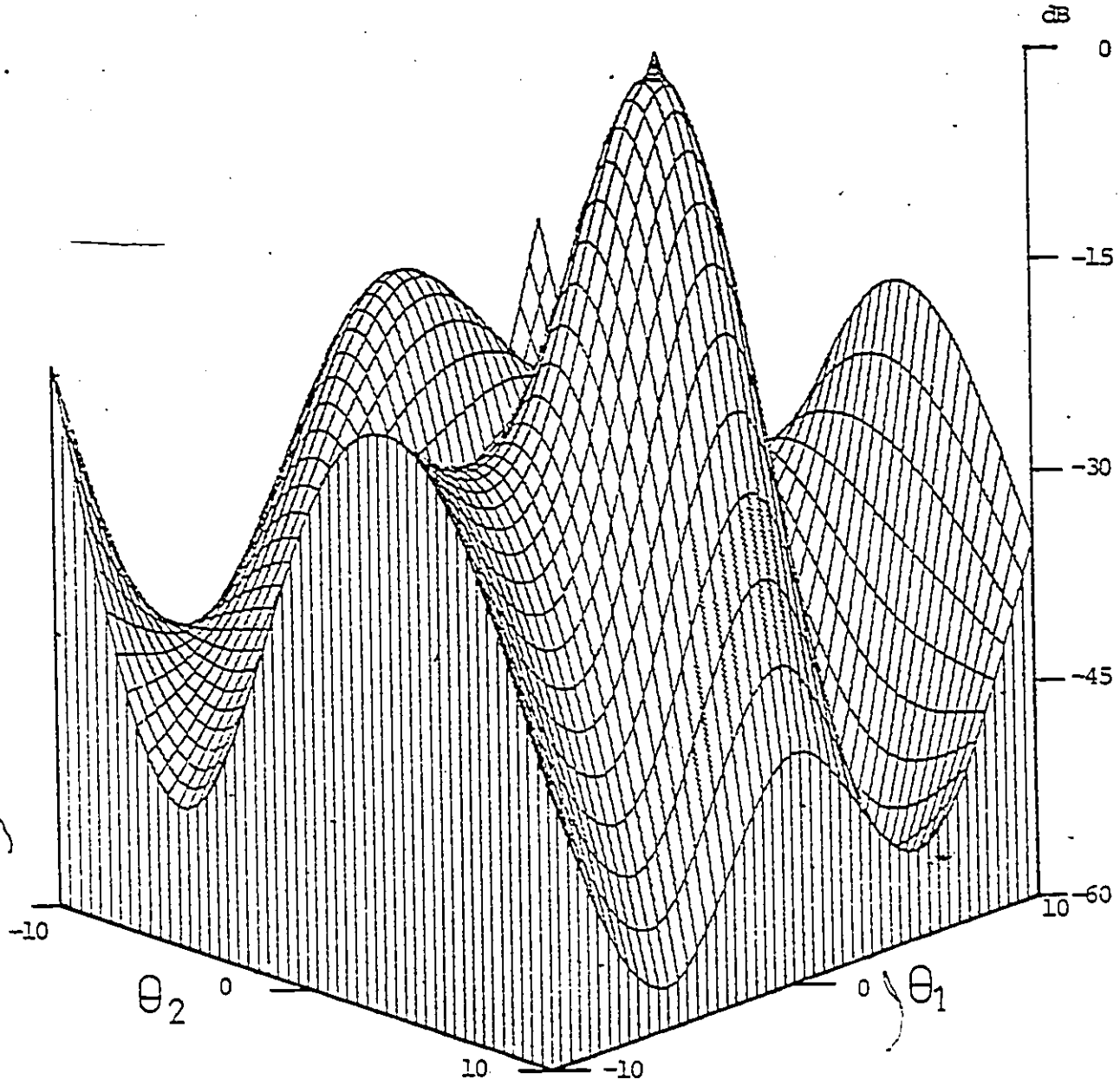

Fig. 4.3 Response pattern of the Mills' cross array antenna for the uniform aperture distribution when the target is at (0,5).

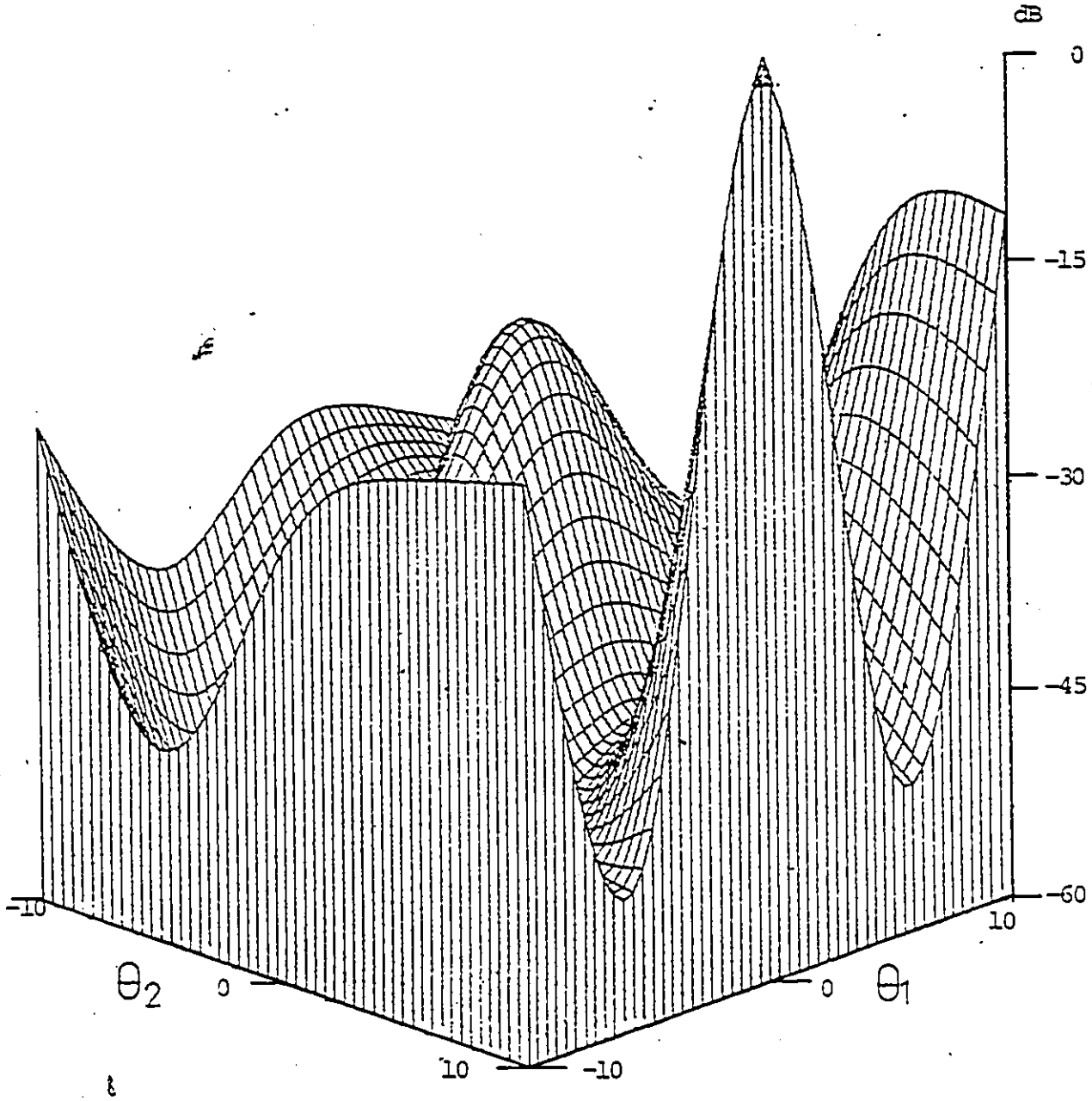

Fig. 4.4 Response pattern of the Mills' cross array antenna for the uniform aperture distribution when the atrget is at (0,10).

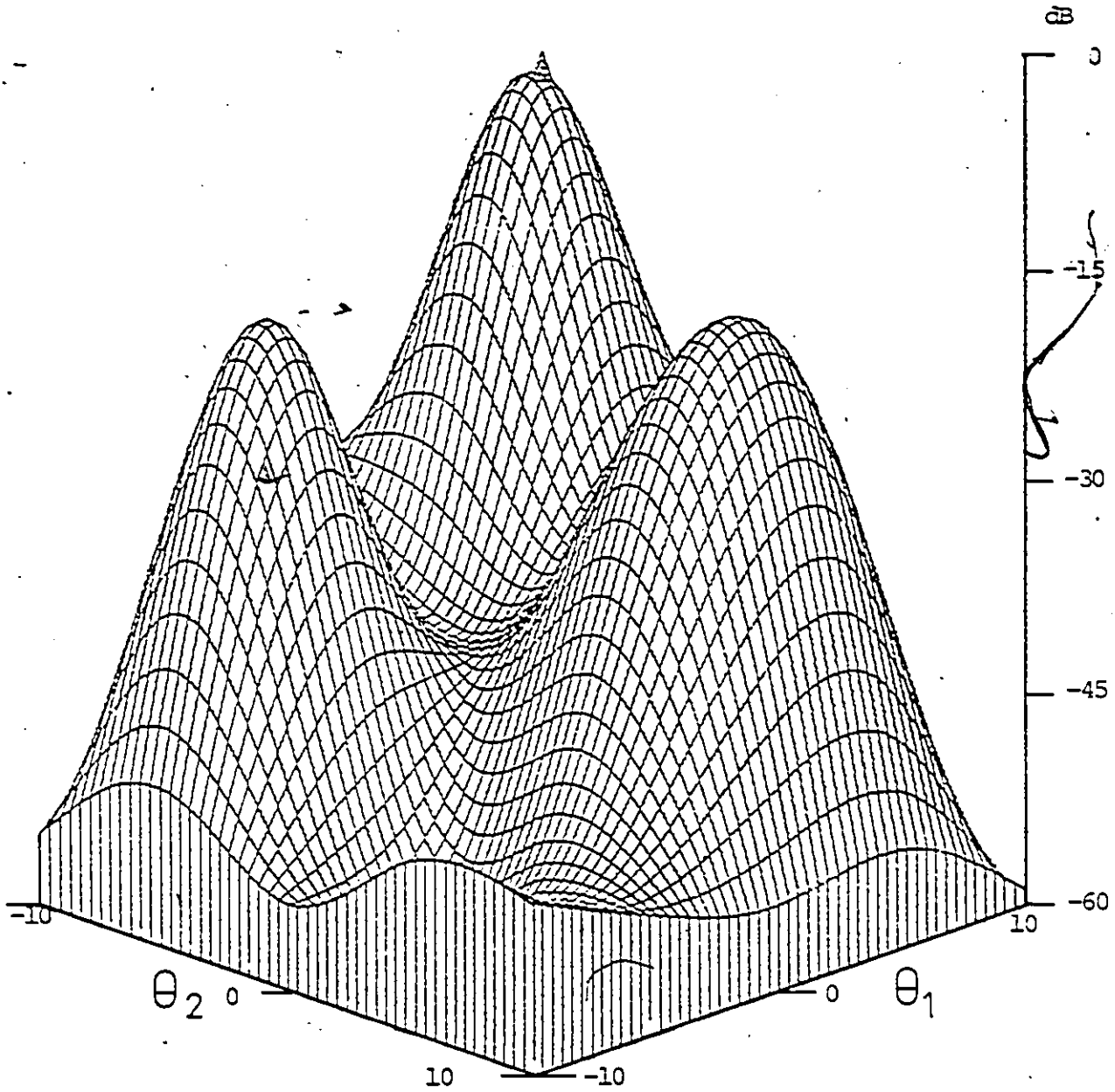

Fig. 4.5 Response pattern of the Mills' cross array antenna for the uniform aperture distribution when the target is at (5,5).

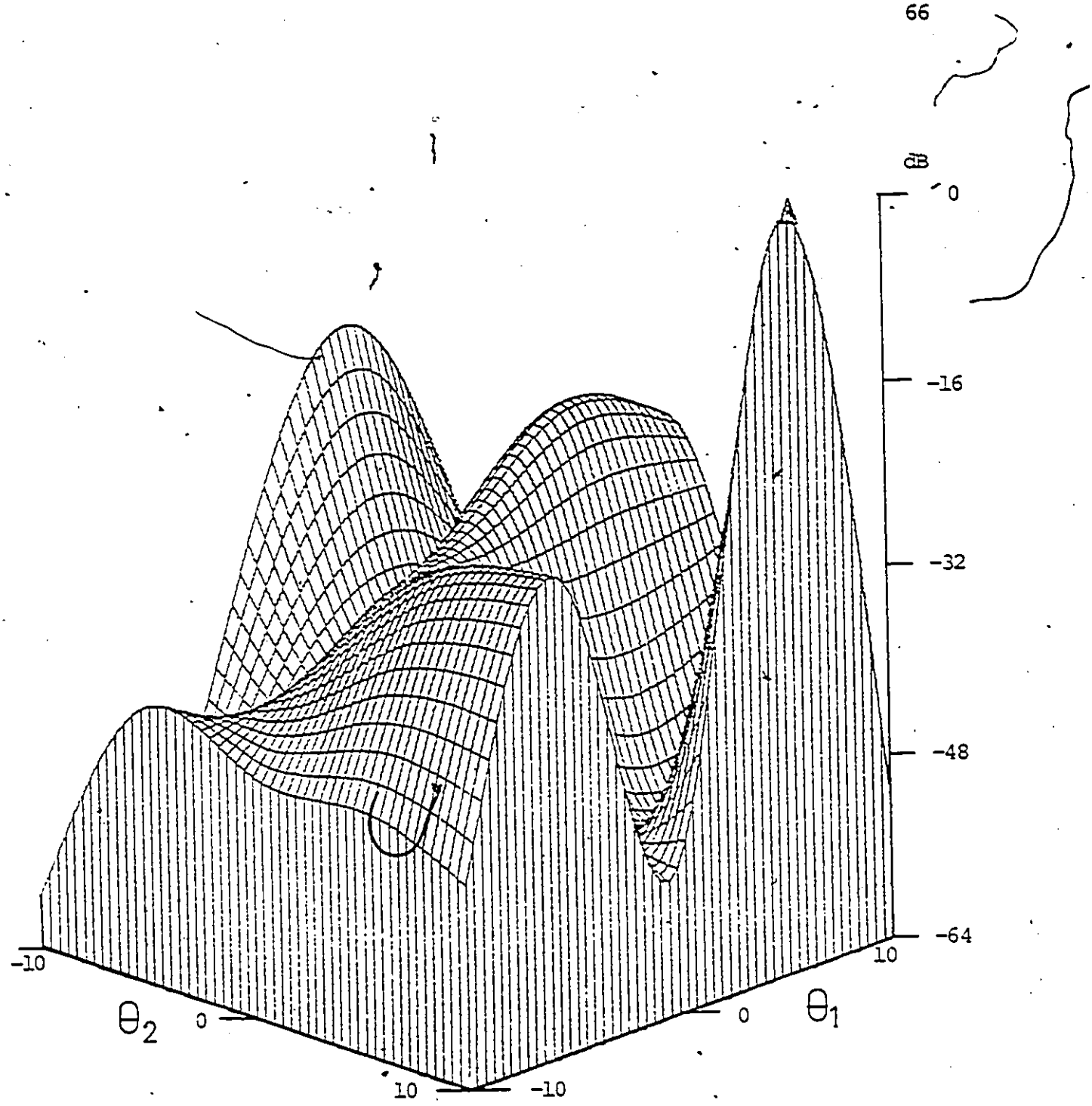

Fig. 4.6 Response pattern of the Mills' cross array antenna for the uniform aperture distribution when the target is at (5,10).

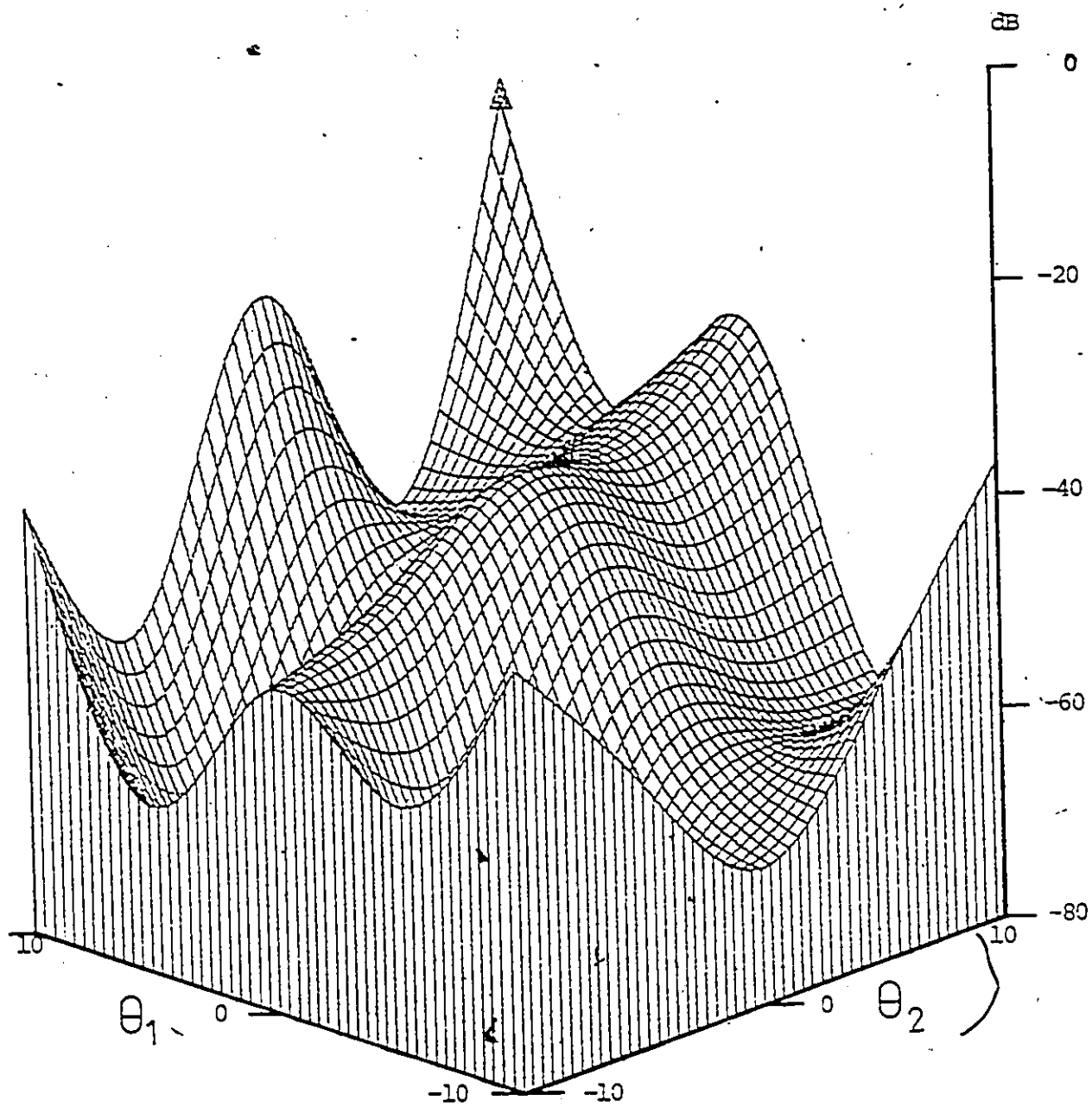

Fig. 4.7 Response pattern of the Mills' cross array antenna for the uniform apreture distribution when the target is at (10,10).

Look direction		Theoretical		Experimental	
θ_1 in degrees	θ_2 in degrees	Beamwidth in degrees	First highest sidelobe level in dB	Beamwidth in degrees	First highest sidelobe level in dB
0	0	2.300	-13.5	2.5	-10
0	5	2.308	-13.5	3.2	- 9
0	10	2.335	-13.5	3.2	- 9
5	5	2.308	-13.5	3.0	-11
5	10	2.335	-13.5	2.7	- 9
10	10	2.335	-13.5	2.6	-11

Table 4.1 Comparison of theoretical and experimental results of the Mills' Cross array antenna for uniform distribution current

that their amplitudes are proportional to the coefficients of a Binomial series, then the sidelobes are completely eliminated, and with an increasing number of radiating elements, the array pattern approaches a Gaussian form. However, for a given number of radiating elements, we may find that the resulting beamwidth is too excessive for practical useage. Another type of aperture weighting is the so-called cosine-on-a-pedestal distribution. However, the best compromize between sidelobe level and beamwidth is achieved by using the Dolph-Chebyshev distribution. This

distribution was proposed by Dolph for the case of broadside arrays, based on the optimum properties of Chebyshev polynomials [22]. For details see Appendix E. Specifically, the elements of the array are weighted according to the Chebyshev polynomial as follows:

$$a_{n+1} = \frac{2}{N}\left[\rho + 2\sum_{i=1}^{N/2-1} T_{N-1}\left(Z_o \cos\frac{i\pi}{N}\right)\cos\frac{i\pi(2n+1)}{N}\right] \quad (4.1)$$

where a_n is the Chebyshev coefficient for the nth element, N is the total number of elements, ρ is the main lobe-to-sidelobe ratio, and

$$T_{N-1}(Z) = \begin{cases} \cos[(N-1)\arccos Z], & |Z| \leq 1 \\ \cosh[(N-1)\operatorname{arccosh} Z], & |Z| > 1 \end{cases} \quad (4.2)$$

and

$$Z_o = \cosh[\{1/(N-1)\}\operatorname{arccosh}\rho] \quad (4.3)$$

These results were derived by Stegan [23] by equating the array space factor to a Fourier Series.

Figures 4.8 to 4.13 show the measured 3-dimensional plots of antenna radiation pattern for the case of an array employing Dolph-Chebyshev distribution for 6 different look directions. In Table 4.2, we have summarized the values of highest side lobe level and half-power beamwidth for the above response patterns, based on theory and measured results.

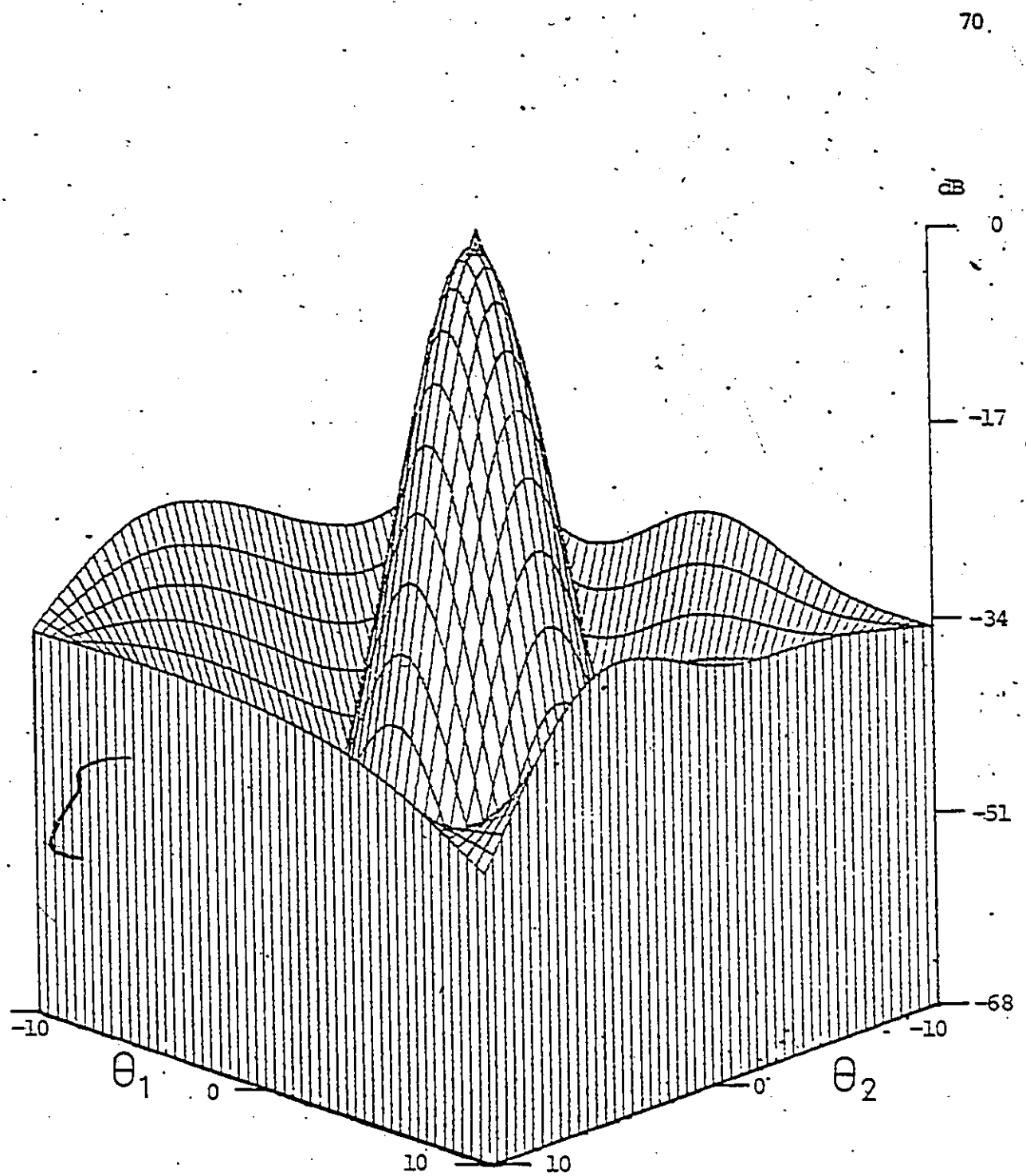

Fig. 4.8 Response pattern of the Mills' cross array antenna for the Dolph-Chebyshev aperture distribution when the target is at (0,0).

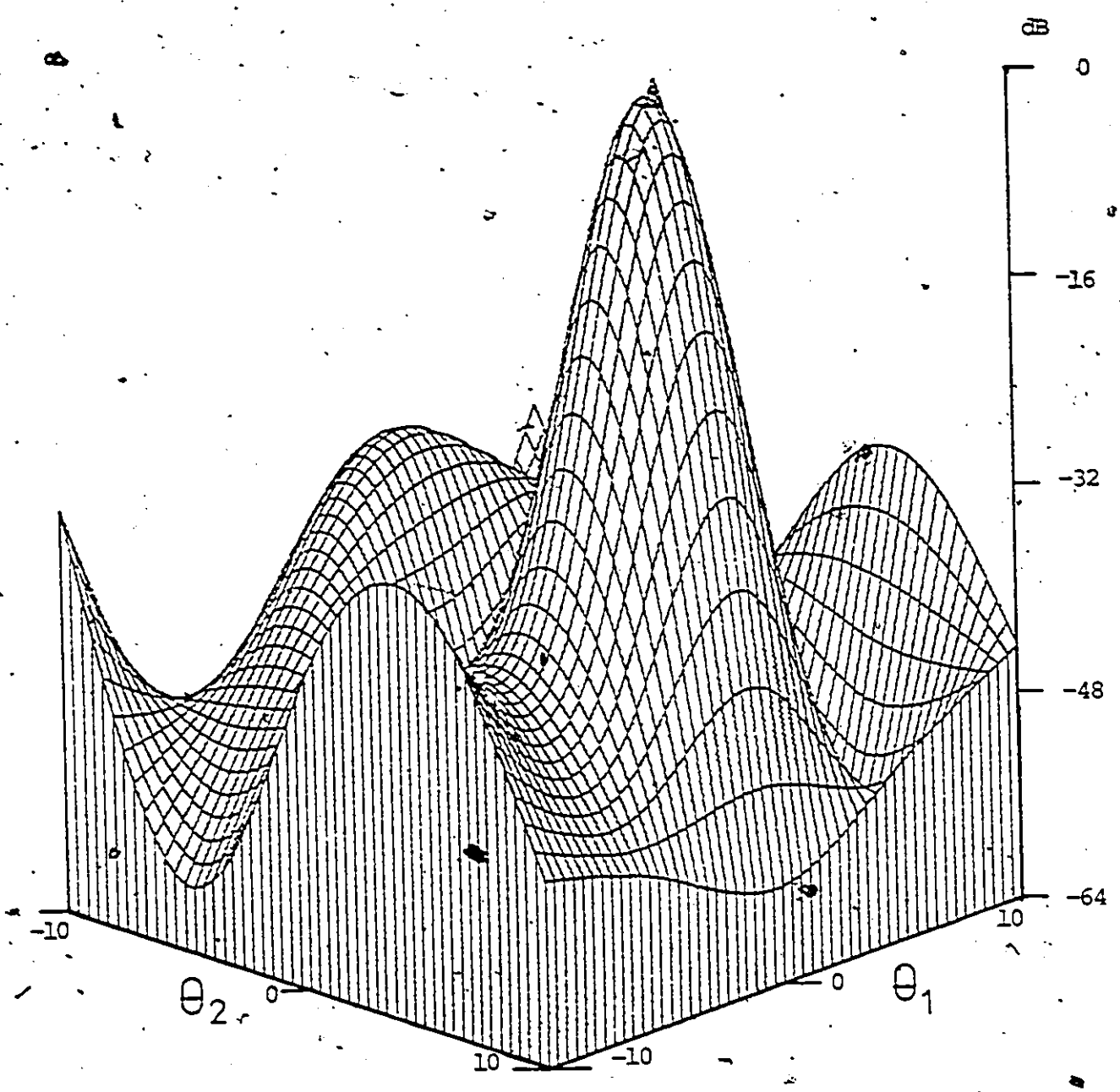

Fig. 4.9 Response pattern of the Mills' cross antenna for the Dolph-Chebyshev aperture distribution when the target is at (0,5).

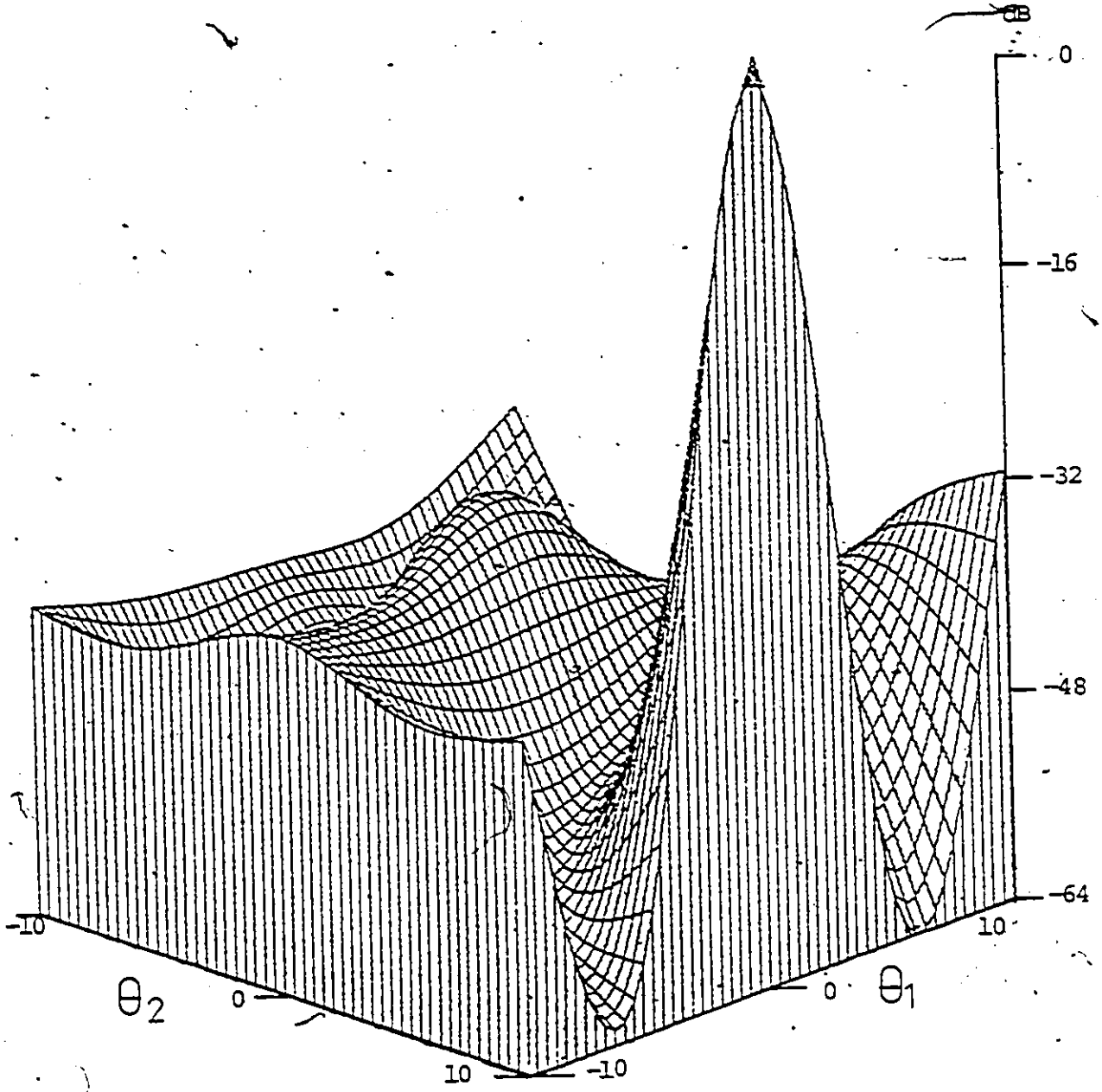

Fig. 4.10 Response pattern of the Mills' cross array antenna for the Dolph-Chebyshev aperture distribution when the target is at (0,10).

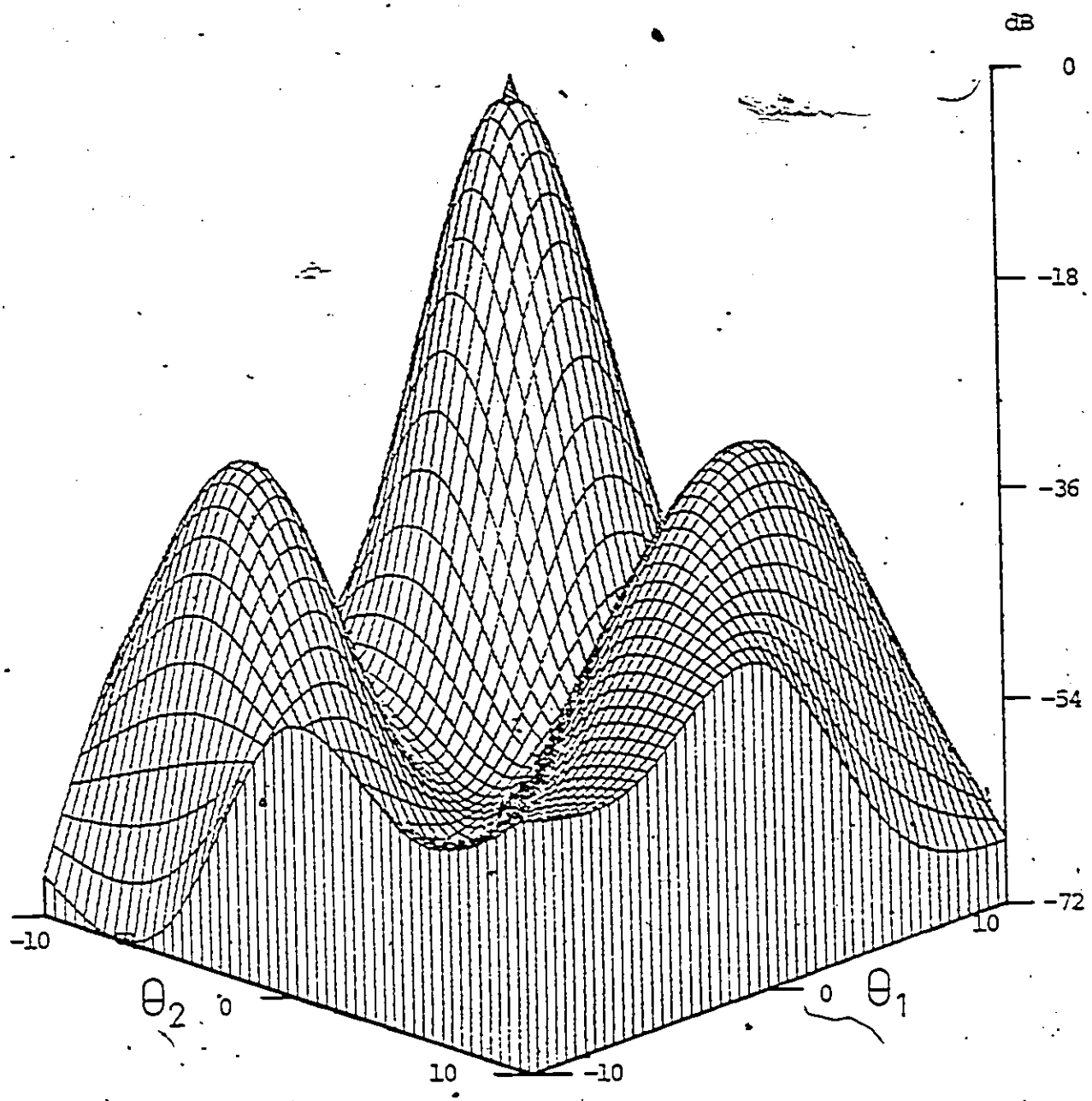

Fig. 4.11 Response pattern of the Mills' cross array antenna for the Dolph-Chebyshev aperture distribution when the target is at (5,5).

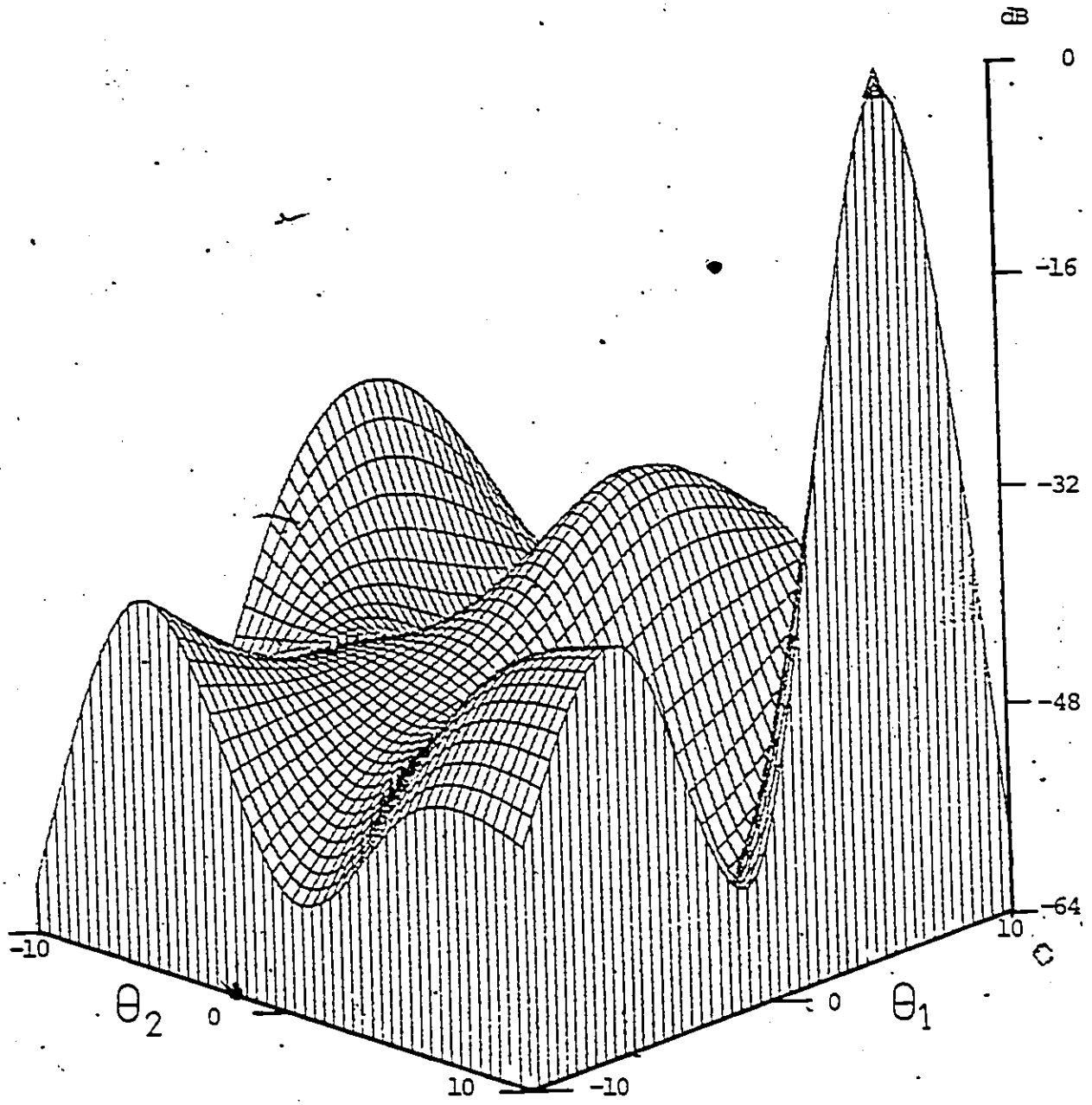

Fig 4.12 Response pattern of the Mills' cross array antenna for the Dolph -Chebyshev aperture distribution when the target is at (5,10).

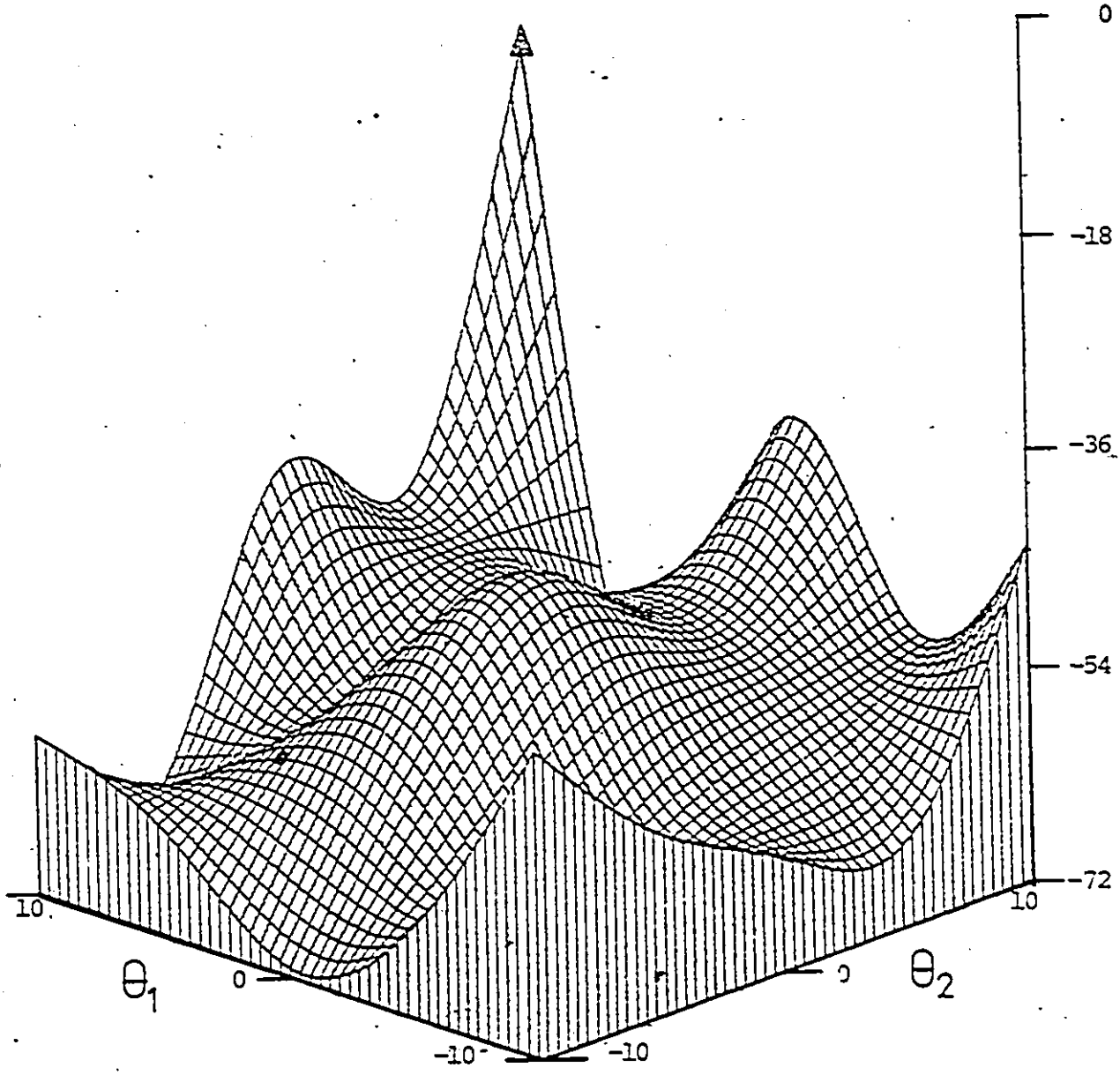

Fig. 4.13 Response pattern of the Mills' cross array antenna for the Dolph - Chebyshev aperture distribution when the target is at (10,10).

Look direction		Theoretical		Experimental	
θ_1 in degrees	θ_2 in degrees	Beamwidth in degrees	First highest sidelobe level in dB	Beamwidth in degrees	First highest sidelobe level in dB
0	0	3.080	-40	3.2	-32
0	5	3.090	-40	3.2	-31
0	10	3.128	-40	3.2	-33
5	5	3.092	-40	3.2	-31
5	10	3.128	-40	3.4	-32
10	10	3.128	-40	2.7	-35

Table 4.2 Comparison of theoretical and experimental results of the Mills' Cross array antenna for Dolph-Chebyshev distribution of current

4.4 Comments on the Experimental Results

In Tables 4.1 and 4.2 we have summarized the theoretical and experimental results corresponding to uniform and Chebyshev types of aperture distribution for different look directions in one quadrant of the scanning sector. By careful examination of the Tables 4.1 and 4.2, we observe that there is close agreement between theory and experiment, certainly with regard to the half-power beam-width. However, the measured values of highest side lobe

level are somewhat higher than the corresponding values deduced from theory. This discrepancy arises because of several factors which have been ignored in the results computed from theory:

(1) The theoretical results are computed assuming an ideal array with isotropic radiators as elements. On the other hand, the horns used in the practical system have elemental patterns of their own.

(2) The theoretical results ignore the effect of mutual coupling between adjacent elements of the array.

(3) The digital baseband processor uses a finite word length (namely, 16 bits), which introduces quantization errors.

(4) The plotting of a three-dimensional antenna pattern from discrete data by employing interpolation is only approximate.

Nevertheless, the experimental results do demonstrate the practical feasibility of using baseband processing with digital hardware to achieve the scanning of a Mills' cross array along prescribed directions in a visible region of interest.

4.5 Summary

Chapter 4 has presented the results of a number of radiation patterns of the Mills' cross array antenna to

targets at different positions in one quadrant of the prescribed scanning sector. The results are presented for both uniform and Chebyshev aperture illuminations. The digital outputs in 16-bits available from the baseband processor are presented in the form of a three dimensional surface projected on a two-dimensional plane by using the method of cubic spline.

The theoretical and experimental results corresponding to uniform and Chebyshev types of aperture distribution for different look directions are summarized in Table 4.1 and 4.2. The results indicate that there is close agreement between theory and experiment, thus confirming the practical feasibility of using baseband processing with digital hardware to achieve raster-like scanning in the prescribed sector.

CHAPTER 5

CONCLUSIONS

The objective of the experiment reported in this thesis was to demonstrate the practical feasibility of scanning a Mills' cross array antenna along prescribed look directions by means of baseband processing with digital hardware, which enables the realization of a high degree of system flexibility. The experimental results presented in Chapter 4 confirm that such a possibility is indeed practical, showing reasonably close agreement with theory.

The baseband processor provides scanning capability of the pencil beam by using time modulation scanning for which it is rather well-suited. The processor offers the following advantages:

(1) The scheme incorporates within-pulse scanning in order to avoid the loss of power in the fan beams outside the area covered by the pencil beam.

(2) The processor eliminates the need for phase-shifters which can be expensive.

(3) It provides flexibility in applying different types of aperture illumination to modify the side lobe structure of the antenna pattern. This is achieved by merely changing the look-up table in the programmable read-only memory.

(4) It provides a simple means of changing the scanning rate of the Mills' cross array antenna.

(5) It employs digital hardware for the processing of baseband signals consisting of in-phase and quadrature components.

To the author's best knowledge, this is the first time that the construction of this form of baseband processor for antenna scanning has been reported in the literature.

It should be mentioned that in a radar application, the duration of the transmitted pulse is typically much shorter, and the number of array elements is typically much larger than the corresponding values used in the experimental study reported in Chapter 4. Nevertheless, with presently available digital devices, there should be no difficulty in constructing a Mills' cross array antenna with 50 x 50 elements (say) to operate with a transmitted radar pulse of 1 μs duration.

APPENDIX A

DISTANCE REQUIREMENT FOR ANTENNA PATTERN MEASUREMENTS

Since the wave emerging from the transmitting antenna is spherical, the phase front across the aperture of the receiving antenna will be flat only when the distance between the transmitting and receiving antennas is infinitely large. For any finite separation, the phase front will be curved. The extent of this curvature or the amount of the phase deviation in terms of separation R and aperture dimension A can be deduced with the aid of Fig. A.1. The path length of the extreme ray OA is R + ΔR, and solving the right triangle OAB, we get

$$(R + \Delta R)^2 = R^2 + (\frac{A}{2})^2 \qquad (A.1)$$

Neglecting $(\Delta R)^2$, we have

$$\Delta R = \frac{A^2}{8R}, \text{ unit of wavelength} \qquad (A.2)$$

Here $\Delta R \times (180/\pi)$ is the maximum phase deviation from a plane, in degrees, for an antenna of aperture A at a distance R from the source.

The effect of such a phase deviation on the measured antenna response can be ascertained by a vector summation of

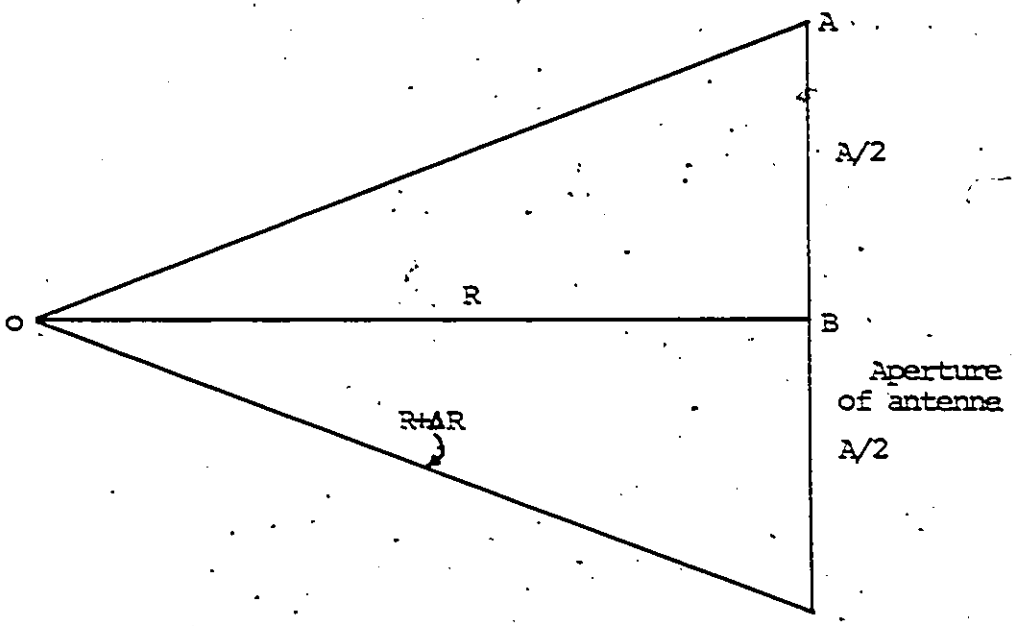

Fig. A.1 Geometry for the derivation of $R \geq \frac{2A^2}{\lambda}$ used in antenna measurements for a phase deviation across the aperture less than $\pi/8$.

the contributions of elementary areas of the antenna aperture. For example, for a phase deviaion of $\pi/8$, the measured gain of an antenna having a uniformly illuminated aperture and a plane wave front will be in error by only 0.1 decibel, which is sufficiently accurate for most antenna work. Specifying, then, that the phase deviation across the antenna aperture be less than $\pi/8$, i.e.,

$$\Delta R \leq \frac{\lambda}{16} \tag{A.3}$$

We obtain

$$R \geq \frac{2A^2}{\lambda} \tag{A.4}$$

APPENDIX B

FRESNEL FIELD OF A FOCUSSED APERTURE

A method of Fraunhofer pattern measurement [18] has been indicated by which the distance between the antennas may be reduced from the usual $2A^2/\lambda$ to values of the order of $0.1\ (A^2/\lambda)$. This reduction may be applied to an antenna in which the aperture may be physically molded about a spherical surface having a radius of curvature less than $2A^2/\lambda$. The possibility of obtaining a true Fraunhofer pattern in the Fresnel region by means of a focussing technique offers a solution applicable to many types of arrays.

It has been shown [18] that the field intensity, at any point $P(x_2, y_2, z_2)$, produced by an aperture which has been molded about a concave spherical surface is given by

$$U_p = F \frac{\exp\,[-jkR]}{R} \int_s f \exp\left[\frac{jk\, x_1 (x_2 - R)}{R}\right] \cdot \exp\,[\, j\, k/R\, (y_1\, y_2 + z_1\, z_2)]\, dS \qquad (B.1)$$

where F = element factor,

f = aperture distribution function,

$k = 2\pi/\lambda$,

λ = wavelength,

exp[jωt] = time dependence

The geometry is shown in Fig. B.1. The term exp [j$kx_1(x_2-R)/R$] is an aberration term and is the factor by which U_p differs from the true Fraunhofer pattern within the limit of Fresnel approximation. From Fig. B.2 it can be seen that $x_{1max} = D = A^2/8R$, since x_1 is usually small; and $(x_2-R) = -R \sin \phi \tan \phi/2$.

Consequently,

$$|k\, x_1\, (x_2-R)/R| \leq (k/R)\ (A^2/8R)\ (R \sin \phi \tan \phi/2)$$

Letting $R = K\cdot A^2/\lambda$,

$$\frac{k\, x_1\, (x_2 - R)}{R} \leq \frac{\pi \sin \phi \tan \phi/2}{4\, K} \qquad (B.2)$$

If the maximum permissible phase error is approximated as $\lambda/16$ so that these measurements are at least as good as the measurements at $R = 2A^2/\lambda$, then $K_{min} = .2 \sin \phi \tan \phi/2$. Thus, the value of K depends on how much of the Fraunhofer pattern it is desired to measure within the specified error.

It can be noted that the phase error as a function of ϕ is zero at $\phi = 0$ and increases to a maximum at $\phi = \pm \pi/2$, while in the case of plane aperture the phase error is maximum at $\phi = 0$ and decreases to zero at $\phi = \pm \pi/2$. Thus, the focussing technique gives minimum error in the vicinity of the main lobe where accuracy is most desirable.

Within the specified error, we then have

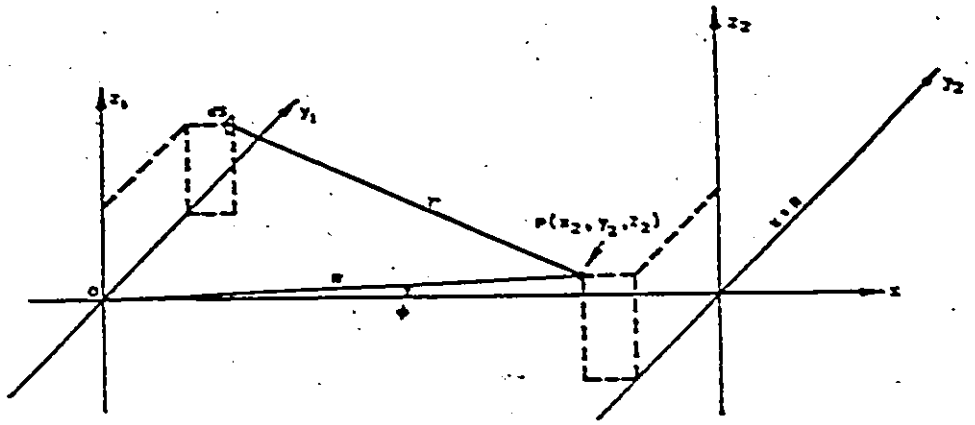

Fig. B.1 Field point geometry.

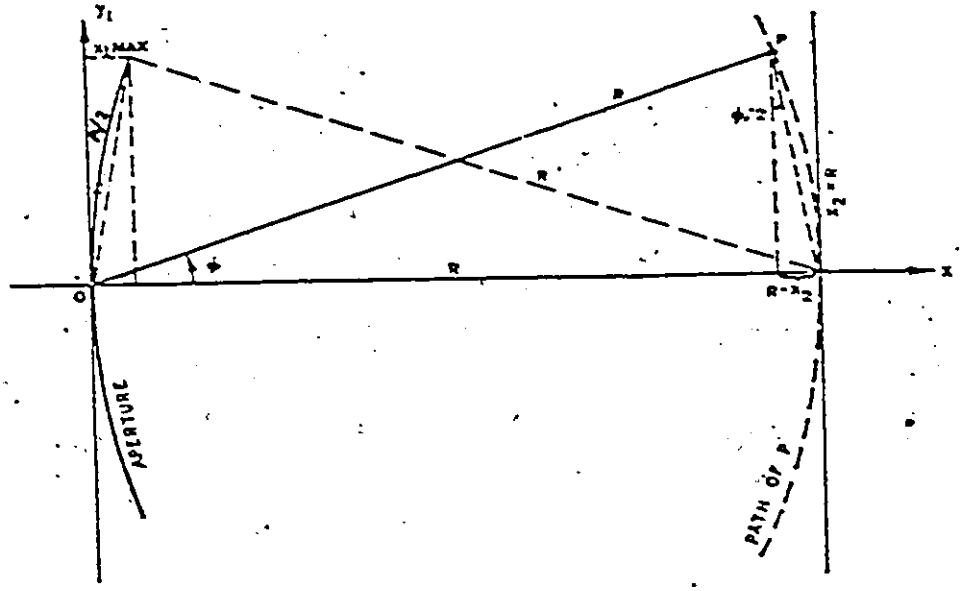

Fig. B.2 Aperture geometry.

$$|U_p| = F/R \int_S f \exp [j\, k/R\, (y_1\, y_2 + z_1\, z_2)]\, dS \qquad (B.3)$$

which is the Fraunhofer field of a plane aperture having a distribution f and element factor F.

APPENDIX C

SMOOTH SURFACE INTERPOLATION

Thin "elastic splines" have long been used by draftsmen to "fair" curves through given set of points in the plane. The close relationship of cubic spline with the draftsman's spline that results from the thin beam approximation leads to many of its important properties and thus motivates much of its application to the problems in numerical analysis. The spline proves to be an effective tool in the elementary processes of interpolation. In the small deflection linear approximation, the segments are even cubic polynomials; hence linearized spline interpolation is a piecewise polynomial method very adaptable to practical numerical computation.

For a function of one variable, linearized spline interpolation defines a function $u(x)$ which assumes given values $u_i = u(x)$ at given points x_i, $i = 0, 1, \ldots, I$, $x_0 < x_1 < x_2 < \ldots < x_I$ and given slopes $\partial u/\partial n$ at the two end points, x_0 and x_I. The interpolating function is a cubic polynomial in each intervals $[x_{i-1}, x_i]$, $i = 1, 0, \ldots, I$.

Bicubic spline interpolation is a two-dimensional analog of "linearized spline interpolation" applicable to

functions of two variables. The analog will also be one of the piecewise polynomial interpolations, defined by polynomial functions on polygonal subdomains having continuous tangent planes across edges connecting adjacent subdomains. Specifically, we suppose that u and $\partial u/\partial n$ are given on the boundary of a rectangular polygon R in the (x,y) plane and that the values of $u(x_i,y_i)$ are also given on a rectangular grid of points. The problem is to interpolate u(x,y) through these given points as smoothly as possible so as to match the given values of u and $\partial u/\partial n$ at the boundary mesh points.

Now assume that the spline curves $u(x,y_j)$ and $u(x_i,y)$ have been calculated in terms of the elevations u_{ij} and slopes $(\partial u/\partial x)_{ij}$ and $(\partial u/\partial y)_{ij}$ at the mesh points (x_i,y_j). We consider the problem of interpolating a surface element z = u(x,y). The whole projection on the (x,y) plane is the rectangle R_{ij}: $x_{i-1} \le x \le x_i$, $y_{j-1} \le y \le y_j$, given all values of u, $\partial u/\partial x$, $\partial u/\partial y$ at the four corners of the rectangle. For each edge of the rectangular surface element, say on x = a, the cubic spline curve defines the height z(x,y) continuously. At the end of each edge, say at (a ± b), the normal slope $\partial z/\partial n = \partial u/\partial x$ is also known. Interpolation is done linearly in $\partial u/\partial x_{(a,y)}$ between these end ponits so as to maintain continuity of slope. Finally,

inside each rectangle R_{ij}, we try to fit a smooth and analytically simple surface to the prescribed boundary values of u and $\partial u/\partial n$.

APPENDIX D

LINEAR ARRAYS: SCANNING CONSIDERATIONS

Let us consider a linear array consisting of N isotropic radiators, excited with equal amplitude and phase. The radiators are separated by distance d as shown in Fig. D.1. Then the field contributions from all the elements, with element O as phase reference, give

$$E_a = \frac{1}{\sqrt{N}} \sum_{n=0}^{N-1} \exp\left[\left(j \frac{2\pi}{\lambda}\right) N d \sin\theta\right] \qquad (D.1)$$

The factor $1/\sqrt{N}$ shows that each element is energized with 1/N of the input power. Adjusting the phase relative to the center of the aperture and normalizing the gain to unity at broadside, $\theta = 0$, give

$$E_a = \left[\exp\left\{\left(-j \frac{2\pi}{\lambda}\right)((N-1)/2)d\sin\theta\right\}\right] \frac{1}{N} \sum_{n=0}^{N-1} \exp\left(j \frac{2\pi}{\lambda} N d \sin\theta\right)$$

$$= \frac{\sin\left[N\pi\ (d/\lambda)\ \sin\theta\right]}{N \sin\left[\pi\ (d/\lambda)\ \sin\theta\right]} \qquad (D.2)$$

E_a gives the radiation pattern with isotropic radiators and is known as the array factor. It is shown in Fig. D.2 for N = 10. The pattern is repetive, and adjacent grating lobes at angles θ_1 and θ_2 are separated by $\pi\ (d/\lambda)\ (\sin\theta_1 - \sin\theta_2) = \pi$.

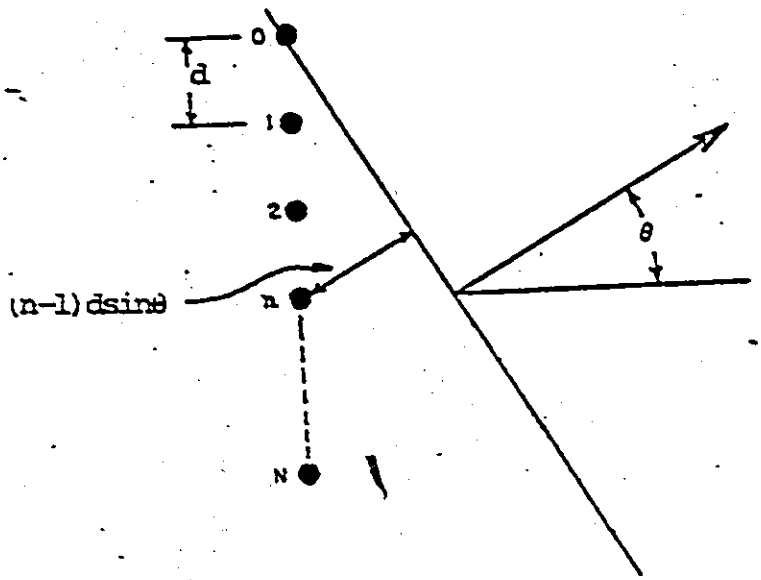

Fig. D.1 Linear phased array with isotropic radiators.

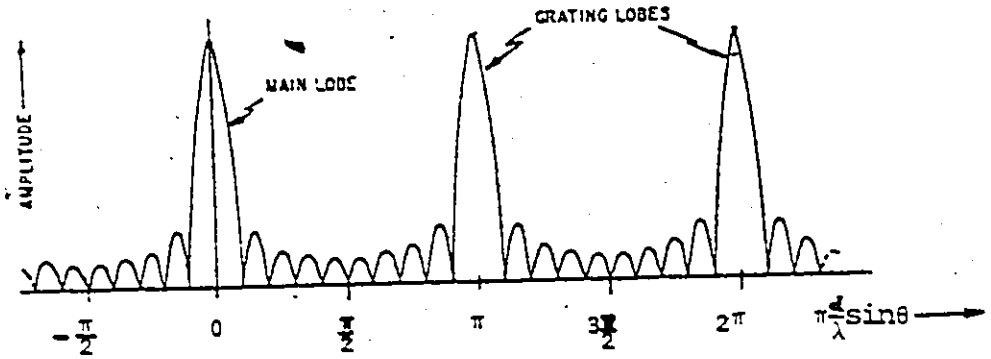

Fig. D.2 Array factor of the linear phased array for N=10.

When the radiating elements are not isotropic but have elemental pattern E_e of their own, the complete radiation pattern E is

$$E = E_a \times E_e$$

$$= E_e \frac{\sin [N\pi (d/\lambda) \sin \theta]}{N \sin [\pi (d/\lambda) \sin \theta]} \qquad (D.3)$$

Now the approximation to the pattern of eq. (D.2) is in the form (sin x)/x:

$$E = \frac{\sin [\pi (A/\lambda) \sin \theta]}{\pi (A/\lambda) \sin \theta} \qquad (D.4)$$

where, A = Nd.

The half-power beamwidth is obtained from eq. (D.4):

$$\theta_B = \frac{0.886}{A/\lambda} \text{ radians} = \frac{50.8}{A/\lambda} \text{ degrees} \qquad (D.5)$$

The first side lobe is 13.5 dB down from the main lobe.

The pattern of the array may be steered to an angle θ_o by applying linearly progressive phase increments from element to element, so that the phase between adjacent elements differs by $(2\pi/\lambda)$ d sin θ_o. Equation (D.2) is then modified, giving the normalized pattern

$$E_a = E_e \frac{\sin[N \pi (d/\lambda) (\sin \theta - \sin \theta_o)]}{N \sin[\pi (d/\lambda) (\sin \theta - \sin \theta_o)]} \qquad (D.6)$$

Equation (D.6) describes the fundamental response of a scanned-array system. The array factor will have only one single major lobe, and grating lobe maxima will not occur at

values of $-90^{\circ} < \theta < +90^{\circ}$ as long as

$$\pi \, d/\lambda \, (\sin \theta - \sin \theta_o) < \pm\pi$$

or

$$\frac{d}{\lambda} < \frac{1}{1 + |\sin \theta_o|} \tag{D.7}$$

which is always true if $d/\lambda < 1/2$. When the scanning is limited, the value of d/λ may be increased, for example, to $d/\lambda < 0.53$ for scanning to a maximum of $\pm 60^{\circ}$ or to $d/\lambda < .59$ for scanning to a maximum of $\pm 45^{\circ}$.

For larger values of d/λ, grating lobes occur at angles θ_1, given by

$$\sin \theta_1 = \sin \theta_0 \pm \frac{n}{d/\lambda} \tag{D.8}$$

where n is an integer.

It is known that the effective aperture of the array antenna is reduced as the array is scanned. Thus correspondingly, the beamwidth is increased to

$$\theta_B \text{ (scanned)} = \frac{\theta_B \text{ (broadside)}}{\cos \theta_o}$$

$$= \frac{0.886}{(A/\lambda) \cos \theta_o} \text{ rad} = \frac{50.8}{(A/\lambda) \cos \theta} \text{ degrees} \tag{D.9}$$

APPENDIX E

DOLPH-CHEBYSHEV OPTIMUM DISTRIBUTION

Consider the case of an array consisting of an even number N of isotropic point sources of uniform spacing d as shown in Fig. E.1. The total field E_N at a large distance in a direction θ is

$$E_N = 2 \sum_{K=0}^{n-1} A_K \cos \left(\frac{2K+1}{2} x\right) \qquad (E.1)$$

where $N = 2(K+1)$, $K = 0, 1, 2, 3, \ldots$

$x = (2\pi/\lambda)\, d \sin \theta$, and

$n = N/2$.

The field pattern of an even number of sources as given by eq. (E.1) is a finite Fourier series. The coefficients A_0, A_1, ... in the series are arbitrary and express the amplitude distribution.

Proceeding now to the Dolph-Chebyshev amplitude distribution, it will be shown that the coefficient of the pattern series eq. (E.1) can be uniqely determined so as to produce a pattern of minimum beamwidth for a specified side-lobe level. Before demonstrating that this is always possible, it will be convenient to consider non-normalized

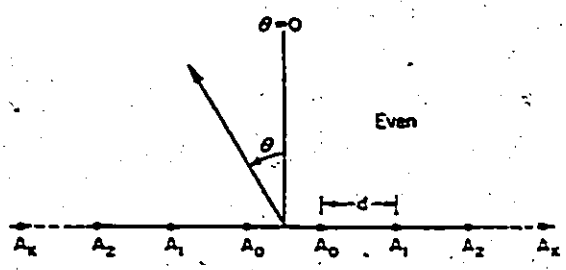

Fig. E.1 Linear phased array with even number of isotropic radiators having equal spacing between successive elements.

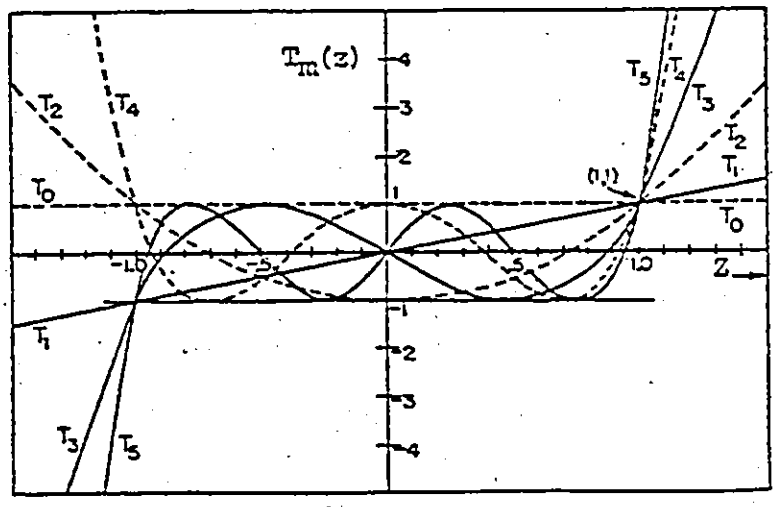

Fig. E.2 Chebyshev polynomials of degree m=0 through m=5.

Chebyshev polynomials. These are defined by

$$T_m(z) = \cos (m \arccos z) \tag{E.2}$$

where $z = \cos x/2$

For particular values of m, the first 8 Chebyshev polynomials are:

$$\left.\begin{aligned} T_0(z) &= 1 \\ T_1(z) &= z \\ T_2(z) &= 2z^2-1 \\ T_3(z) &= 4z^3-3z \\ T_4(z) &= 8z^4-8z^2+1 \\ T_5(z) &= 16z^5-20z^3+5z \\ T_6(z) &= 32z^6-48z^4+18z-1 \\ T_7(z) &= 64z^7-112z^5+56z^3-7z \end{aligned}\right\} \tag{E.3}$$

We note in eq. (E.3) that the degree of the polynomial is the same as the value of m. The roots of the polynomials occur when

$$\cos (m \arccos z) = 0$$

or when $$m \arccos z = (2K-1)\ \pi/2 \tag{E.4}$$

where $K = 1, 2, 3, \ldots$

The roots of z, designated z', are thus

$$z' = \cos [(2K-1)\ \pi/2m] \tag{E.5}$$

Thus eq. (E.1) expresses the field pattern of a symmetric in-phase equispaced linear array of N isotropic point sources and is a polynomial of degree equal to the number of sources less 1. If we now set the array polynomial given by

eq. (E.1) equal to the Chebyshev polynomial of like degree (m = N-1) and equate the array coefficients to the coefficients of Chebyshev polynomial, then the amplitude distribution given by these coefficients is a Chebyshev distribution and the field pattern of the array corresponds to the Chebyshev polynomial of degree N-1.

The Chebyshev polynomials of degree m=0 through m=5 are presented in Fig. E.2. Referring to Fig. E.2, the following properties of the polynomials are deduced:

(1) All polynomials pass through the point (1,1)

(2) For values of z in the range $-1 \leq z \leq +1$, the polynomials all lie between ordinate values of +1 and -1. All roots occur between $-1 \leq z' \leq +1$, and all maximum values in this range are ±1.

We now describe Dolph's method of applying the Chebyshev polynomial to obtain an optimum pattern. Let the ratio of the main-lobe to the side-lobe level be specified as ρ. That is,

$$\rho = \frac{\text{Main-lobe maximum}}{\text{side-lobe level}}$$

Next solve the equation $T_m(z_o) = \rho$ for z_o. A change of scale is made by introducing a new abscissa w where

$$w = z/z_o \qquad \text{(E.6)}$$

Then the constraint that z must be restricted to the range $-1 \leq z \leq +1$ can be fulfilled by putting

$$w = \cos x/2 \qquad \text{(E.7)}$$

where now the range of w is restricted to $-1 \leq w \leq +1$. The pattern polynomial (E.1) may now be expressed as a polynomial in w. The final step is

$$T_{N-1}(z) = E_N \tag{E.8}$$

The coefficients of the array polynomial are then obtained from (E.8) yielding the Dolph-Chebyshev amplitude distribution which is optimum for a specified side-lobe level.

As the number of elements becomes large, the equations become unwieldy, not only because of the number of calculations, but also the accuracy required in intermediate calculations. By using a Fourier analysis approach in the calculations, the computations simplify and, as a bonus, also require less computational accuracy. This procedure is applied in our case as discussed in Chapter 4.

REFERENCES

[1] B.Y. Mills and A.G. Little, "High resolution aerial system of new type", Australian J. of Physics, Vol. 6, p. 272, 1953.

[2] B.Y. Mills, "Cross type radio telescopes", Proc. I.R.E. (Australia), Vol. 24, p. 132, 1963.

[3] P.D. Kalachov, "Some radio telescopes in the U.S.S.R.", Proc. I.R.E. (Australia), Vol. 24, p. 237, 1963.

[4] A. Braccesi and M. Ceccarelli, "The Italian cross radio telescope", Nuovo Cimento [10] Vol. 23, p. 208, 1962.

[5] R.J. Wislez and R. Gonze, "Radio heliograph of the royal observatory of Belgium", Electrical Communications, Vol. 49, No. 3, p. 218, 1974.

[6] B.R. Slattery, "Use of Mills' cross receiving arrays in radar system", Proc. I.E.E., Vol. 113, No. 11, p. 1712, 1966.

[7] D.E.N. Davies, "High data rate radars incorporating array signal processing and thinned arrays", IEEE International Radar Conference, p. 371, 1975.

[8] M.A. Johnson, "Phased array beam steering by multiplex sampling", Proc. I.E.E.E., Vol. 56, No. 11, p. 1801, 1968.

[9] H.E. Shanks, "A new technique for electronic scanning", I.R.E. Trans. on Antennas and Propagation, Vol. AP-9, p. 162, 1961.

[10] R.C. Hansen, "Microwave scanning antennas", Vol. III, Array Systems, Academic Press, Inc., New York, 1966.

[11] M.I. Skolnik, "Radar Handbook", McGraw-Hill, Inc., New York, 1970.

[12] A. Ishimaru and H.S. Tuan, "Theory of frequency scanning of antennas", I.R.E. Trans. Vol. AP-10, p. 144, March 1962.

[13] J. Blass, "The multidirectional antenna: A new approach to steered beams", I.R.E. Intern. Conv. Record, Vol. 8, Pt. 1, p. 48, 1960.

[14] J.C. Bulter, "Multiple beam antenna", Sanders Associates, Nashua, New Hampshire, Memo RF-3849, January 1960.

[15] J.P. Shelton and K.S. Kelleher, "Mltiple beam from linear arrays", I.E.E.E. Trans., Vol. AP-9, p. 154, March 1961.

[16] S. Haykin, "Communication Systems", John Wiley and Sons, Inc., New York, 1978.

[17] S. Haykin, "Performance analysis of a radar signal processing system with continuous electronic array processing", Information Sciences, Vol. 13, p. 201, 1977.

[18] R.W. Bickmoke, "Fraunhofer pattern measurement in the Fresnel region", Canadian J. of Physics, Vol. 35, p. 1299, 1957.

[19] S. Haykin and H. Rahman, "Digital baseband processing of a Mills' cross array antenna", accepted for publication in the Canadian Journal of Electrical Engineers, 1979.

[20] J. Ahlberg, E. Nilson and J. Walsh, "The theory of splines and their applications", Academic Press, New York, 1967.

[21] J.D. Kraus, "Antennas", McGraw-Hill Book Company, New York, 1950.

[22] C.L. Dolph, "A current distribution which optimizes the relationship between beamwidth and side-lobe levels", Proc. I.R.E., Vol. 34, p. 335, 1946.

[23] R.J. Stegan, "Excitation coefficients and beamwidths of Tchebycheff arrays", Proc. I.R.E., Vol. 41, p. 1671, 1953.

[24] D.G. Tucker, "Multiplicative array in radio-astronomy and sonar systems", Journal Brit. Instn. Radio Engrs., Vol. 25, p. 113, 1963.